Ultra-High Performance Concrete: 4 PDH

Four (4) Continuing Education Hours
Course #CV1605

Approved Continuing Education for Licensed Professional Engineers

EZ-pdh.com
Ezekiel Enterprises, LLC
301 Mission Dr. Unit 571
New Smyrna Beach, FL 32170
800-433-1487
support@ez-pdh.com

Course Description:

The Ultra-High Performance Concrete course satisfies four (4) hours of professional development.

The course is designed as a distance learning course that provides a comprehensive overview of UHPC, covering its materials and production methods, mechanical and durability properties, structural behavior, and applications in bridges. It consolidates global research, field implementations, and technical specifications to inform future use of UHPC in infrastructure projects.

Objectives:

The primary objective of this course is to educate engineers, designers, and infrastructure stakeholders on the research, development, and deployment of UHPC, enabling informed decision-making and promoting the adoption of this high-performance material in modern bridge construction.

Grading:

Students must achieve a minimum score of 70% on the online quiz to pass this course. The quiz may be taken as many times as necessary to successfully pass and complete the course.

A copy of the quiz questions is attached to the last pages of this document.

TABLE OF CONTENTS

CHAPTER 1. INTRODUCTION

BACKGROUND

Ultra-high performance concrete (UHPC) in its present form became commercially available in the United States in about 2000. The Federal Highway Administration (FHWA) began investigating the use of UHPC for highway infrastructure in 2001 and has been working with State transportation departments to deploy the technology since 2002. This work has led to the use of UHPC in several bridge applications, including precast, prestressed girders; precast waffle panels for bridge decks; and as a jointing material between precast concrete deck panels and girders and between the flanges of adjacent girders. At the same time, research work has been underway at several universities in the United States.

In Canada, the first UHPC bridge was constructed in 1997. This pedestrian bridge consists of a precast, post-tensioned space truss. At least 26 bridges have been built in Canada using UHPC in one or more components.

In Germany, a 12 million euro research program, begun in 2005, has just been completed. That program, funded by the German Research Foundation, involved 34 research projects at more than 20 research institutes in Germany. The purpose of the program was to elaborate on the basic knowledge so that reliable technical standards could be developed. The goal was to make UHPC a reliable, commonly available, economically feasible, regularly applied material. Several bridges that use UHPC have been built in Germany.

In 2002, the first recommendations on the use of UHPC in structures were published in France. This initial document addressed mechanical properties, structural design, and durability. Since 2002, several bridges have been built in France using UHPC. In 2009, several papers published in French recommended updates to the recommendations. A similar set of design recommendations was developed for use in Japan.

Other countries with bridges using UHPC include Australia, Austria, Croatia, Italy, Japan, Malaysia, the Netherlands, New Zealand, Slovenia, South Korea, and Switzerland. The literature search identified more than 90 completed bridges using UHPC in one or more components. A major research program is currently underway in South Korea to investigate the use of UHPC in cable-stayed bridges. It is obvious, therefore, that UHPC is receiving worldwide attention.

The evolution of UHPC into its present formulation has been a gradual process occurring over many years. Several papers have summarized this development. Naaman and Wille identified many of the significant advances in the technology over the last 5 decades. Buitelaar summarized the early developments in the Netherlands and Denmark. Richard and Rossi described the developments in France.

As part of its ongoing activities to implement UHPC in the United States, FHWA has requested a state-of-the-art report about the research, development, and deployment of UHPC. This document reports what has been done and looks ahead to what needs to be done to achieve appropriate applications in the U.S. highway infrastructure.

OBJECTIVE

The objective of this report is to document the state of the art with regard to the research, development, and deployment of UHPC components within the U.S. highway transportation infrastructure. In addition, because much of the development and initial deployment of UHPC has occurred internationally, the report also documents work completed outside the U.S. highway sector. In addition, the report addresses what is needed to allow future wider implementation of UHPC.

SCOPE

Similar to how Graybeal defines it, this document defines UHPC-class materials as cementitious-based composite materials with discontinuous fiber reinforcement, compressive strengths above 21.7 ksi (150 MPa), pre-and post-cracking tensile strengths above 0.72 ksi (5 MPa), and enhanced durability via their discontinuous pore structure. However, the published literature does not always include sufficient information to determine whether the tested materials conformed to this definition. Unless an obvious reason existed to exclude an article, it is included in this report.

The authors identified more than 600 references relevant to this report. Some topics are described in more than one article by the same or similar combinations of authors. Some articles also provide updates on previous articles on the same topic. For this report, the most comprehensive documents readily available and written in English are used for most of the cited references. The other articles are listed in the Bibliography. Based on this approach, the majority of articles in this report come from the following publications:

- FHWA reports.
- Proceedings of the International Symposium on Ultra High Performance Concrete, Kassel, Germany, September 2004.
- Proceedings of the Second International Symposium on Ultra High Performance Concrete, Kassel, Germany, March 2008.
- Proceedings of the International Workshop on Ultra High Performance Fibre Reinforced Concrete—Designing and Building with UHPFRC: State of the Art Development, November 2009, Marseille, France.
- Proceedings of Hipermat 2012 3rd International Symposium on UHPC and Nanotechnology for High Performance Construction Materials, Kassel, Germany, March 2012.

The articles published in the proceedings of the international meetings are usually summaries of the research or applications and written in English. As such, the articles do not contain sufficient information for use in developing design guides or specifications. For more details, the articles

often refer to a full report written in a language other than English. Use of these reports requires either a comprehension of the other language or an English translation.

TERMINOLOGY

Various terms are used to refer to cementitious-based composite materials with high compressive strength and enhanced durability. These include the following:

- Compact reinforced composite (CRC).
- Densified small-particle (DSP) concrete.
- Fiber-reinforced high-performance concrete (FRHPC).
- High-performance fiber reinforced cement composite (HPFRCC).
- Macro defect free (MDF) concrete.
- Multi-scale fiber-reinforced concrete (MSFRC).
- Reactive powder concrete (RPC).
- Steel fibrous cement-based composite (SFCBC).
- Ultra-high performance concrete (UHPC).
- Ultra-high performance fiber-reinforced cementitious composite (UHPFRCC).
- Ultra-high performance fiber-reinforced concrete (UHPFRC).
- Ultra-high strength concrete (UHSC).
- Ultra-high strength cement-based composite.
- Ultra-high strength cementitious material.
- Ultra-high strength fiber-reinforced cementitious composite.

In addition, various patterns of hyphens are used to form compound adjectives. For this report, the product is generally called ultra-high performance concrete or UHPC unless it is necessary to differentiate the different types. Descriptions of some of the different types are provided by Rossi. Although calling the different types by a single name may not be technically correct, it simplifies understanding the available information.

This report also refers to conventional concrete. Conventional concrete is composed of cementitious materials, fine and coarse aggregates, water, and admixtures. Compressive strengths are assumed to be in the range of 4 to 8 ksi (28 to 55 MPa).

SUSTAINABILITY

Few articles have been published about the sustainability of UHPC compared with the number published about its material and engineering properties. Several authors have addressed the topic because of the increasing requirement to consider sustainability.

Racky determined that the energy and raw material consumption to produce a square reinforced column made of UHPC were 74 and 58 percent, respectively, of the quantities required for a Grade 40/50 (6/7 ksi) column. He also pointed out that UHPC had greater frost and deicing salt resistance, a lower rate of carbonation, and greater chloride resistance than conventional concretes. Consequently, highway structures made with UHPC will have lower maintenance and

repair costs in the future compared with conventional concrete bridges. However, sufficient data were lacking to perform realistic life cycle cost analyses.

Schmidt and Jerebic reported that the energy demanded for production of 1.3 yd^3 (1 m^3) of UHPC was approximately double that for conventional concrete. However, when the total energy demand to construct the Gaertnerplatz bridge using UHPC and steel tubes was compared with the energy demand for an equivalent conventional prestressed concrete bridge, the increase was reduced to 25 percent. The largest component of energy was for the production of the steel tubes. If the steel tubes could be replaced by UHPC tubes, the estimated energy demand would drop by about 50 percent. When the CO_2 contributions from construction to the greenhouse effect were considered, the UHPC-steel combination had the largest value, the UHPC tube the lowest, and the prestressed concrete bridge was intermediate.

Sedran, Durand, and de Larrard reported that UHPC called Ceracem could be crushed and separated into sand and fibers. The recycled sand could then be used as a replacement for river sand in self-leveling concrete with no loss of fluidity and no decrease in compressive strength.

Stengel and Schießl reported that the environmental impact of UHPC production was mainly caused by the production of the steel fibers, portland cement, and high-range water-reducing admixtures. The effect of heat curing UHPC was not taken into account. In another study, life-cycle assessments of bridge structures were made using German standard Deutsches Institut für Normung (DIN) ISO 14040 ff. The research concluded that the environmental impact of structures made with state-of-the-art UHPC was up to 2.5 times greater than with conventional concrete. The environmental impact could be decreased by reducing the amount of portland cement, steel fibers, and high-range water-reducing admixtures in the UHPC.

COSTS

The initial unit quantity cost of UHPC far exceeds that of conventional concrete. Consequently, applications have focused on optimizing its use by reducing concrete member thickness, changing concrete structural shapes, or developing solutions that address shortcomings with existing non-concrete structural materials. As discussed in chapter 5, UHPC is a very durable product, and structures that use it are expected to have a longer service life and require less maintenance than structures built with conventional concrete.

Piotrowski and Schmidt conducted a life cycle cost analysis of two replacement methods for the Eder bridge in Felsberg, Germany. One method used precast UHPC box girders filled with lightweight concrete. The second method used conventional prestressed concrete bridge members. Although the UHPC had higher initial costs, the authors predicted the life cycle cost over 100 years would be less for the UHPC bridge.

CHAPTER 2. MATERIALS AND PRODUCTION

CONSTITUENT MATERIALS AND MIX PROPORTIONS

UHPC formulations often consist of a combination of portland cement, fine sand, silica fume, high-range water-reducing admixture (HRWR), fibers (usually steel), and water. Small aggregates are sometimes used, as well as a variety of chemical admixtures. Different combinations of these materials may be used, depending on the application and supplier. Some of these are described in this section.

The UHPC used most often in North America for both research and applications is a commercial product known as Ductal®. Table 1 shows a typical composition of this material.

Table 1. Typical composition of Ductal®

Material	lb/yd^3	kg/m^3	Percentage by Weight
Portland Cement	1,200	712	28.5
Fine Sand	1,720	1,020	40.8
Silica Fume	390	231	9.3
Ground Quartz	355	211	8.4
HRWR	51.8	30.7	1.2
Accelerator	50.5	30.0	1.2
Steel Fibers	263	156	6.2
Water	184	109	4.4

Aarup reported that CRC, developed by Aalborg Portland in 1986, consisted of large quantities of steel fibers (2 to 6 percent by volume), large quantities of silica fume, and a water-binder ratio of 0.16 or lower.

The following recommendations for mix proportions were developed for use with commercially available constituent materials:

- Cement with a moderate fineness and C_3A content significantly lower than 8 percent.
- Sand-to-cement ratio of 1.4 for a maximum grain size of 0.8 mm (0.03 inches).
- Silica fume with very low carbon content at 25 percent of the weight of cement.
- Glass powder with a median particle size of 67 x 10^{-6} inches (1.7 μm) at 25 percent of the weight of cement.
- High-range water-reducing admixture.
- Water-cement ratio of about 0.22.
- Steel fibers at 2.5 percent by volume.

By optimizing the cementitious matrix for compressive strength, packing density, and flowability; using very high strength, fine-diameter steel fibers; and tailoring the mechanical bond between the steel fiber and cement matrix, 28-day compressive strengths in excess of 30 ksi (200 MPa) on 2-inch (50-mm) cubes were achieved with no heat or pressure curing. In addition, a tensile strength of 5.0 ksi (34.6 MPa) at a strain of 0.46 percent was obtained. The UHPC incorporated materials available in the United States and was mixed in a conventional concrete mixer. Table 2 gives one mix proportion.

Table 2. UHPC mix proportions of CRC by weight

Material	Proportions
Portland Cement	1.0
Fine Sand[1]	0.92
Silica Fume	0.25
Glass Powder	0.25
HRWR	0.0108
Steel Fibers	0.22 to 0.31
Water	0.18 to 0.20

[1] Maximum size of 0.008 inches (0.2 mm)

Habel et al. reported that it is possible to produce self-consolidating UHPC for use in precast products and cast-in-place (CIP) applications without requiring heat or pressure treatment during curing. This mix design was further developed and implemented in a research program conducted by Kazemi and Lubell.

Holschemacher and Weißl investigated different mix proportions to minimize material costs without sacrificing the beneficial properties of UHPC. Through careful selection of aggregates, cement type, cementitious materials, inert filler, and HRWR, it was possible to produce UHPC with good workability and moderate material costs.

The concept of combining different size molecular admixtures to facilitate UHPC dispersion was studied by Plank et al.

The possibility of replacing silica fume in UHPC with metakaolin, pulverized fly ash, limestone microfiller, siliceous microfiller, micronized phonolith, or rice husk ash has been investigated. The use of local materials rather than proprietary products has also been pursued.

Schmidt et al. reported two mix proportions for a bridge in Germany. The first mix contained 1,854 lb/yd^3 (1,100 kg/m^3) of cement, 26-percent silica fume as a percentage of the cement content, quartz sand, 6 percent steel fibers by volume, HRWR, and a water-binder ratio of 0.14. The second mix contained 2,422 lb/yd^3 (1,437 kg/m^3) of cement and 9-percent steel wool and steel fibers combined.

Collepardi et al. reported that the replacement of fine ground quartz sand with an equal volume of well-graded natural aggregate with a maximum size of 0.3 inches (8 mm) did not change the compressive strength at the same water-cement ratio.

Coppola et al. investigated the influence of high-range water-reducing admixture type on the compressive strength. They reported that acrylic polymer admixtures allowed the use of lower water-cement ratios and resulted in higher compressive strengths compared with naphthalene and melamine admixtures.

In a study of the durability of UHPC, Teichmann and Schmidt used the mix proportions shown in table 3. Mix 1 had a maximum aggregate size of 0.32 inches (8 mm) provided by the sand. Mix 2 had a maximum aggregate size of 0.32 inches (8 mm) provided by the basalt.

Table 3. UHPC mix proportions from Teichmann and Schmidt

	Mix 1		Mix 2	
Material	**lb/yd^3**	**kg/m^3**	**lb/yd^3**	**kg/m^3**
Cement	1,235	733	978	580
Silica Powder	388	230	298	177
Fine Quartz 1	308	183	503	131
Fine Quartz 2	0	0	848	325
HRWR	55.5	32.9	56.2	33.4
Sand	1,699	1,008	597	354
Basalt	0	0	1,198	711
Steel Fibers	327	194	324	192
Water	271	161	238	141
Water-Binder Ratio	0.19	0.19	0.21	0.21

Researchers at the U.S. Army Corps of Engineers Engineer Research and Development Center have reported on a UHPC-class material referred to as Cor-Tuf. The proportions of this UHPC are presented in table 4.

Table 4. UHPC mix proportions of Cor-Tuf by weight

Material	**Proportions**
Portland Cement	1.0
Sand	0.967
Silica Flour	0.277
Silica Fume	0.389
HRWR	0.0171
Steel Fibers	0.310
Water	0.208

Researchers led by Rossi at the Laboratoire Central des Ponts et Chaussees (LCPC) in Paris developed a UHPC-class material referred to as CEMTEC$_{multiscale}$. The proportions of this UHPC are presented in table 5.

Table 5. UHPC mix proportions for CEMTEC$_{multiscale}$

Material	lb/yd^3	kg/m^3
Portland Cement	1,770	1,050
Sand	866	514
Silica Fume	451	268
HRWR	74	44
Steel Fibers	1,446	858
Water	303	180

MIXING AND PLACING

Graybeal has summarized the mixing of UHPC as follows:

> Nearly any conventional concrete mixer will mix UHPC. However, it must be recognized that UHPC requires increased energy input compared to conventional concrete, so mixing time will be increased. This increased energy input, in combination with the reduced or eliminated coarse aggregate and low water content, necessitates the use of modified procedures to ensure that the UHPC does mot overheat during mixing. This concern can be addressed through the use of a high-energy mixer or by lowering the temperatures of the constituents and partially or fully replacing the mix water with ice. These procedures have allowed UHPC to be mixed in conventional pan and drum mixers, including ready-mix trucks.

Mixing times for UHPC range from 7 to 18 minutes, which are much longer than those of conventional concretes. This impedes continuous production processes and reduces the capacity of concrete plants. Mixing time can be reduced by optimizing the particle size distribution, replacing cement and quartz flower by silica fume, matching the type of HRWR and cement, and increasing the speed of the mixer. The mixing time can also be reduced by dividing the mixing process into two stages. High-speed mixing for 40 seconds is followed by low-speed mixing for 70 seconds, for a total time of about 2 minutes.

The method of placing UHPC has an influence on the orientation and dispersion of the fibers. The orientation did not affect the first cracking load but had an effect of up to 50 percent on the ultimate tensile strength in bending. The highest strengths were achieved when placement was made in the direction of the measured tensile strength. Stiel et al. reported significant differences between horizontally and vertically cast beams when tested in three-point bending. The fibers in the vertically cast beams were aligned in layers normal to the casting direction. As a result, the splitting and flexural strengths were only 24 and 34 percent of the corresponding values for the horizontally cast beams. However, in a 39-inch (1-m)-thick slab, the fibers were arranged randomly. The orientation of the fibers did not have a significant effect on the compressive strength and modulus of elasticity.

Graybeal has summarized the placement of UHPC as follows:

> The placement of UHPC may immediately follow mixing or be delayed while additional mixes are completed. Although the dwell time prior to the initiation of the cement hydration reactions can be influenced by factors such as temperature and chemical accelerators, it frequently requires multiple hours before UHPC will begin to set. During extended dwell time, the UHPC should not be allowed to self-desiccate.
>
> Casting of fiber-reinforced concretes requires special considerations in terms of placement operations. UHPCs tend to exhibit rheological behaviors similar to conventional self-consolidating concretes, thus possibly necessitating additional form preparation but also allowing for reduced during-cast efforts. Internal vibration of UHPC is not recommended due to fiber reinforcement, but limited external form vibration can be engaged as a means to facilitate the release of entrapped air.

For the UHPC beams used on the Route 624 bridge over Cat Point Creek in Richmond, VA, the contractor was required to use a plant that was prequalified for UHPC production, and a representative from the UHPC producer was required to be present. The UHPC was mixed in 4-yd^3 (3-m^3) batches in an 8-yd^3 (6-m^3) twin shaft mixer and discharged into a ready-mixed concrete truck for delivery. About 20 to 25 minutes were required to load the mix, mix the UHPC, and discharge the mixer.

During discharge from the truck, cement balls were observed in the mix. This was attributed to exposure of the bags to moisture during storage. The mix was discharged into one end of the beam and allowed to flow. Only limited external vibration was applied for 1 or 2 seconds.

CURING

Curing of UHPC considers two distinct components, specifically temperature and moisture. As with any cementitious composite material, maintaining an appropriate temperature is critical to achieving the desired rate for the cementitious reactions. In addition, given the low water content in UHPC, eliminating loss of internal water by sealing the system or maintaining a high humidity environment is also critical.

The curing of UHPC occurs in two phases. Given that UHPC tends to exhibit a dormant period prior to initial setting, the initial curing phase consists of maintaining an appropriate temperature while precluding moisture loss until setting has occurred and rapid mechanical property growth is occurring. The second curing phase may or may not include elevated temperature conditions and a high moisture environment, depending on whether accelerated attainment of particular material characteristics is desired.

Graybeal reported on an extensive program to determine material properties of UHPC using four different post-set curing procedures. These involved steam curing at 194 °F (90 °C) or 140 °F (60 °C) for 48 hours, starting about 24 hours after casting; steam curing at 194 °F (90 °C),

starting after 15 days of standard curing; and curing at standard laboratory temperatures until test age.

These three steam-curing methods increased the measured compressive strengths and modulus of elastic, decreased creep, virtually eliminated drying shrinkage, decreased chloride ion penetrability, and increased abrasion resistance. The enhancements achieved by the lower steam temperature and delayed steam curing were slightly less than achieved by steam curing at the higher temperature. The specimens steam cured at 194 °F (90 °C) after 24 hours reached their full compressive strengths within 4 days after casting. Chapter 3 of this report presents more details of the test results.

More recent work by Graybeal has focused on characterizing the performance of ambient-cured UHPC. This research stems from the recognition that accelerated curing in a steam environment is frequently not practical and also that the ambient-cured properties of UHPC are appropriate for many applications.

Ay compared the compressive strength of 4-inch (100-mm) cubes cured by the following three methods:

- Curing in water until 1 hour before testing.
- Curing in water for 5 days followed by air curing.
- Sealing the cubes in plastic sheeting and then storing them at 68 °F (20 °C) until tested.

The UHPC cubes stored in water followed by air curing had slightly higher compressive strengths than cubes cured by the other two methods.

The compressive strength of UHPC can be increased considerably by using post-set heat curing. Heinz and Ludwig showed that the heat curing at various temperatures between 149 and 356 °F (65 and 180 °C) produced 28-day compressive strengths as high as 41 ksi (280 MPa) compared with strengths of 25 and 27 ksi (178 and 189 MPa) when cured at 68 °F (20 °C). Higher curing temperatures resulted in higher compressive strengths. In addition, the strengths at the end of the curing period at about 48 hours after casting were about the same as the corresponding 28-day strengths. The authors also concluded that curing at 194 °F (90 °C) presented no danger of delayed ettringite formation.

Schachinger et al. observed that initial curing at 68 °F (20 °C) for 5 days, followed by heat curing at 122 to 149 °F (50 to 65 °C), was the most favorable combination to achieve high strengths at ages up to 28 days. Compressive strengths in the range of 36 to 43.5 ksi (250 to 300 MPa) were achieved at ages of 6 to 8 years.

Heinz et al. achieved compressive strengths higher than 29 ksi (200 MPa) at an age of 24 hours after 8 hours storage at 68 °F (20 °C) followed by 8 hours at 194 °F (90 °C) in water. Longer periods of initial storage or heat treatment resulted in higher strengths when ground-granulated blast-furnace slag was included in the UHPC. The authors obtained the highest strengths by including fly ash and autoclaving the UHPC for 8 hours at 300 °F (150 °C).

Massidda et al. showed that autoclaving at a temperature of 356 °F (180 °C) and 145 psi (1 MPa) with saturated steam produced higher compressive strengths and flexural strengths compared with specimens cured at 68 °F (20 °C).

QUALITY CONTROL TESTING

Quality control tests for UHPC in the United States have generally used the same or similar tests as those used for conventional concrete or mortar with or without modifications. Both fresh and hardened concrete properties are measured.

The flow of UHPC is frequently measured using ASTM C1437—Standard Test Method for Flow of Hydraulic Cement Mortar. This test method is intended for use with mortars exhibiting plastic to flowable behavior, and thus it is frequently appropriate for fresh UHPC. In this test, both initial flow and dynamic flow are measured. The test is completed immediately after mixing to assess consistency among mixes and appropriateness for casting. On the Route 24 bridge over Cat Point Creek, a minimum dynamic flow of 9 inches (230 mm) was sought for satisfactory workability.

As different versions of UHPC are developed for different applications, alternate workability tests will be needed. For stiffer, non-self-consolidating UHPC, the ASTM C143—Standard Test Method for Slump of Hydraulic-Cement Concrete may be appropriate. Scheffler and Schmidt have reported that development of stiff UHPC formulations for applications such as pavement whitetopping is feasible.

The initial and final setting times of UHPC can be longer than those observed for many conventional cementitious materials. The set times are heavily influenced by the curing temperature. Graybeal measured initial setting times ranging from 70 minutes to 15 hours for different UHPC formulations using the American Association of State Highway and Transportation Officials (AASHTO) T 197 test method for penetration resistance. The corresponding final setting times ranged from 5 to 20 hours.

Compressive strength testing of UHPC is frequently completed using a modified version of ASTM C39—Standard Test Method for Compressive Strength of Cylindrical Concrete Specimens. The test method is modified to include an increased load rate of 150 psi/second (1 MPa/second) in response to the high compressive strength that UHPC exhibits. Appropriate cylinder end preparation is critical because non-flat or non-parallel end surfaces can cause a reduction in observed compressive strength. End surface preparation for cylinders with early age compressive strengths below 12 ksi can be completed using multiple methods, including capping according to ASTM C617. Higher strength cylinders should have their ends ground to within 0.5 degrees.

Smaller cylinders have been shown to provide strengths equivalent to traditional size cylinders. Graybeal reported that 3- by 6-inch (76- by 152-mm) cylinders exhibited similar strengths to 4- by 8-inch (102- by 203-mm) cylinders while allowing for the use of a significantly reduced testing machine capacity. Use of 2- by 4-inch (51- by 102-mm) cylinders was not recommended because of the increased dispersion present in the results.

Research has demonstrated that the ASTM C109—Standard Test Method for Compressive Strength of Hydraulic Cement Mortars (Using 2-inch (50-mm) Cube Specimens) can also be applied to UHPC. Graybeal reported that 2-inch, 2.8-inch, and 4-inch cubes exhibited compressive strengths up to approximately 7 percent greater than those observed from 3- by 6-inch and 4- by 8-inch (76- by 152-mm and 102- by 203-mm) cylinders. Similar findings were reported by Alhborn and Kollmorgen.

On the U.S. Route 6 bridge over Keg Creek in Pottawatomie County, IA, UHPC was used in the longitudinal and transverse joints between the concrete deck panels. The Special Provisions for the project required the contractor to cast twelve 3- by 6-inch (75- by 150-mm) cylinders for verification of concrete compressive strength. Three cylinders were to be tested to verify 10.0 ksi (69 MPa) at 96 hours, three to verify 15.0 ksi (103 MPa) for opening the bridge to traffic, and three at 28 days. The remaining three specimens were treated as reserves. Specimens were required to have their ends ground to 1 degree planeness.

For field-cast UHPC joints, the New York State Department of Transportation (NYSDOT) also requires the casting of twelve 3- by 6-inch (75- by 150-mm) cylinders for testing in sets of three. One set is tested at 4 days, one set at 28 days, one set is to be supplied to the NYSDOT, and one set is treated as reserve.

For qualification testing of the proposed UHPC mix, NYSDOT requires that a minimum of sixty-four 2-inch (50-mm) cubes be cast. Testing ages are 4, 7, 14, and 28 days. Minimum compressive strengths of 14.3 ksi (100 MPa) at 4 days and 21.8 ksi (150 MPa) at 28 days are required.

Frölich and Schmidt investigated the repeatability and reproducibility of tests methods for fresh UHPC. They observed that the values of the measured fresh properties were influenced by the time of measurement, mixing equipment, laboratory conditions, operator, and air-void content. The authors concluded that quality control tests should be made 30 minutes after the start of mixing and that flowable consistency should be measured using the slump flow test.

SUMMARY OF MATERIALS AND PRODUCTION

The constituent materials of UHPC generally consist of portland cement, fine sand, ground quartz, HRWR, accelerating admixture, steel fibers, and water. As a class, UHPCs have high cementitious materials contents and very low water-cementitious materials ratios. UHPC can be mixed in conventional mixers but the UHPC mixing time is longer than for conventional concrete. The method of placing UHPC has an influence on the orientation and dispersion of the fibers, which influences the tensile properties of the UHPC. The properties of UHPC are affected by the method, duration, and type of curing. As with conventional concrete, heat curing accelerates the development of strength and related properties. Delaying the application of heat for several days can enhance the measured properties, although it may not be compatible with the rapid production in precasting operations. Smaller size cylinders have been used in quality control for measurement of compressive strengths.

CHAPTER 3. MECHANICAL PROPERTIES

This chapter summarizes information about the various mechanical properties that are relevant to the structural design of UHPC components.

It is important to note that the dispersion and orientation of the fiber reinforcement are critical parameters that influence the mechanical behavior of UHPC. The fiber reinforcement serves to resist tensile stresses in the UHPC component both before and after tensile cracking of the UHPC matrix. Post-cracking mechanical response of UHPC is particularly susceptible to degradation from disadvantageous fiber dispersion and/or orientation. Mixing and placing methods can affect the hardened UHPC mechanical response and thus must be appropriately coordinated to ensure acceptable mechanical performance.

COMPRESSIVE STRENGTH

Compressive strength is an important property in the design of any concrete structure. It is also the property that is most frequently measured. As discussed in the previous chapter, cylinder and cube compression test methods used for conventional concrete are appropriate for the determination of UHPC compressive strength. Minor modifications to the test and analysis methods may be required.

Graybeal reported the compressive strengths of nearly 1,000 specimens subjected to the following four different curing conditions:

a. Steam curing at 194 °F (90 °C) and 95-percent relative humidity for 48 hours starting about 24 hours after casting.
b. Steam curing at 140 °F (60 °C) for 48 hours starting about 24 hours after casting.
c. Steam curing at 194 °F (90 °C) for 48 hours starting about 15 days after casting.
d. Curing under laboratory conditions (73 °F (23 °C) and ambient humidity).

Most tests were conducted on 3- by 6-inch (76- by 152-mm) cylinders with the ends ground so that they were parallel within 1 degree. Tests generally used the procedures of ASTM C39, except the loading rate was increased to 150 psi/second (1 MPa/s), and a 6.5-inch (165-mm)-diameter spherical bearing plate was used.

The average measured compressive strengths at 28 days for six cylinders cured using methods a, b, c, and d were 28.0, 24.8, 24.8, and 18.3 ksi (193, 171, 171, and 126 MPa), respectively. Density of the UHPC ranged from 150 to 156 lb/ft^3 (2,400 to 2,500 kg/m^3). Within each curing regime, there was a slight increase in compressive strength as the density increased.

Graybeal also investigated the effect of cylinder and cube size on the measured compressive strength using 2- by 4-inch, 3- by 6-inch, 4- by 8-inch, and 3- by 6.5-inch (51- by 102-mm, 76- by 152-mm, 103- by 203-mm, and 76- by 165-mm) cylinders and 2- and 3.94-inch (51- and 100-mm) cubes.

The measured strengths were all within 8 percent of the control 3- by 6-inch (76- by 152-mm) cylinder strength. The cubes had compressive strengths about 5 percent higher than the cylinders.

Similar results were also observed by Orgass and Klug. The smaller cylinders and cubes had a larger standard deviation. Magureanu et al. reported that 3.9-inch (100-mm) cubes had a 20-percent lower measured compressive strength than 2.0-inch (50-mm) cubes.

Graybeal also indicated that loading rates between 35 and 245 psi/seconds (0.24 and 1.7 MPa/seconds) had no noticeable effect on the measured compressive strength, modulus of elasticity, and Poisson's ratio.

Skazlic et al. investigated the effect of cylinder size on the compressive strength of 10 different UHPC mixtures. Cylinder diameters were 2.75, 4, and 6 inches (70, 100, and 150 mm) with a length-to-diameter ratio of 2:1. Assuming a 4- by 8-inch (100- by 200-mm) cylinder as a standard, the authors proposed conversion factors of 1.05 to 1.15 for strengths measured on 2.75- by 5.5-inch (70- by 140-mm) cylinders and 0.85 to 0.95 for strengths measured on 6- by 12-inch (150- by 300-mm) cylinders.

Based on a regression analysis of the data for the particular mix tested, Graybeal determined that the compressive strength gain of UHPC cured under standard laboratory conditions can be represented by the equation in figure 1 for any time after 0.9 days.

$$f'_{ct} = f'_c \left[1\text{-}exp\left(- \left(\frac{t - 0.9}{3} \right)^{0.6} \right. \right.$$

Figure 1. Equation. Compressive strength gain at any age after casting from Graybeal

where:
f'_{ct} = UHPC compressive strength at age t days
f'_c = UHPC compressive strength at 28 days
t = time after casting in days

Graybeal recently completed a follow-on study focused on a readily available UHPC that is formulated for use in field-cast connection applications. A single mix design was cured at 105 °F (41 °C), 73°F (23 °C), and 50 °F (10 °C) to assess the rate of compressive mechanical property development. The time to initiation of compressive mechanical strength gain is provided in figure 2. The relationship between curing temperature and compressive strength is provided in figure 3. The fitting parameters relevant to figure 3 are in table 6.

$$t_{start} = \frac{2.8}{\sqrt{T}}$$

Figure 2. Equation. Relationship between curing temperature and initiation of rapid compressive strength gain from Graybeal

where:
t_{start} = time of initiation of strength gain in days
T = curing temperature in degrees Celsius

$$f'_{c,t} = f'_{c,28d}\left(1 - e^{-\left(\frac{t-t_{start}}{a}\right)^{b}}\right)$$

Figure 3. Equation. Relationship between time after mix initiation and compressive strength as a function of curing temperature from Graybeal

where:
f'_{c28d} = compressive strength at 28 days
$f'_{c,t}$ = compressive strength at time t in days after mix initiation
t_{start} = time of initiation of strength gain in days
a = fitting parameter in days
b = dimensionless fitting parameter

Table 6. Parameters relevant to equation presented in figure 3

Curing Regime	T (°C)	$f'_{c,28d}$ (ksi)	a (days)	b
105°F (41 °C)	41	24.5	0.25	0.25
73° F (23 °C)	23	24	1.0	0.30
50° F (10 °C)	10	22.5	4.0	0.50

Note: 1 ksi = 6.89MPa and °F = 1.8 X °C + 32

Kazemi and Lubell also investigated compressive strength as a function of time after casting. The response of a locally sourced UHPC from central Canada was found to correspond to the relationship in figure 3, with a equal to 4 and b equal to 0.5 or 0.6 depending on the fiber content.

Schmidt and Fröhlich reported that irregularities in the loaded surface of specimens tested in compression caused a more pronounced decrease in the measured compressive strength in UHPC than was evident with conventional concrete.

Tests of UHPC in axial compression at elevated temperatures showed that the measured compressive strength decreases as the concrete temperature at testing increases. However, some or all of the strength is recovered after the specimens cool down.

Richard reported that compressive strengths as high as 80 ksi (550 MPa) can be achieved at atmospheric pressure and heat treating at 480 °F (250 °C). With pressure, compressive strengths as high as 117 ksi (810 MPa) are possible. With conventional production capabilities and curing at 194 °F (90 °C), strengths of 40 ksi (280 MPa) can be achieved.

Tests of UHPC under biaxial compression have been reported by Curbach and Speck and Leutbecher and Fehling.

Additional compressive strength data are available in many of the publications about research and applications of UHPC. These data indicate that the initiation of strength gain and subsequent rate of strength gain depend on the particular UHPC constituent materials, mix proportions, and the curing conditions.

TENSILE STRENGTH

In conventional structural design for concrete bridges, the tensile strength of concrete is assumed to be zero in reinforced concrete design and often taken as $6\sqrt{f_c'}$ in prestressed concrete girder design.

The tensile strength of UHPC is higher than that of conventional concrete, and UHPC can exhibit sustained tensile strength after first cracking. The results of tests for tensile strength of UHPC, therefore, often report a value of first cracking strength as well as a peak post-cracking strength. Consequently, tensile strength takes on increasing importance as a property to consider in design.

An example tensile stress-strain response obtained from a readily available UHPC containing 2 percent by volume steel fiber reinforcement was captured by Graybeal and is shown in figure 4. The results shown were developed as part of a study.

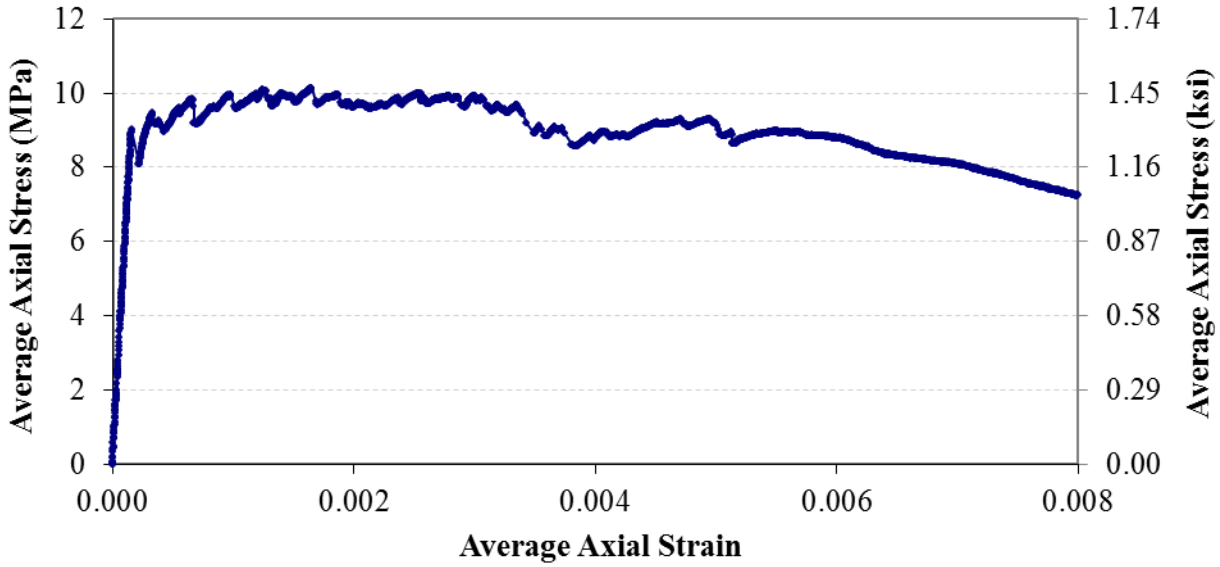

Figure 4. Graph. Tensile stress-strain response of UHPC

Graybeal has proposed the idealized tensile stress-strain response shown in figure 5. This response is based on direct tension tests of two UHPCs with multiple fiber contents. It is proposed as a conceptual illustration of the precracking and postcracking tensile stress-strain response of strain-hardening fiber reinforced concretes, such as UHPC. The behavior is divided into four phases. Phase I is elastic behavior. Phase II is the phase wherein multiple tightly spaced cracks form in the UHPC matrix. The cracks occur individually as the stress in the matrix exceeds the matrix cracking strength. Phase III begins at the strain level where additional cracking between existing cracks is unlikely. Individual cracks widen in this phase. Lastly, Phase IV begins when an individual crack has reached its strain limit and the fibers bridging that crack begin to pull out of the matrix. In a strain-hardening fiber-reinforced concrete, the fiber bridging strength where localization occurs is greater than the cracking strength where multicracking occurs.

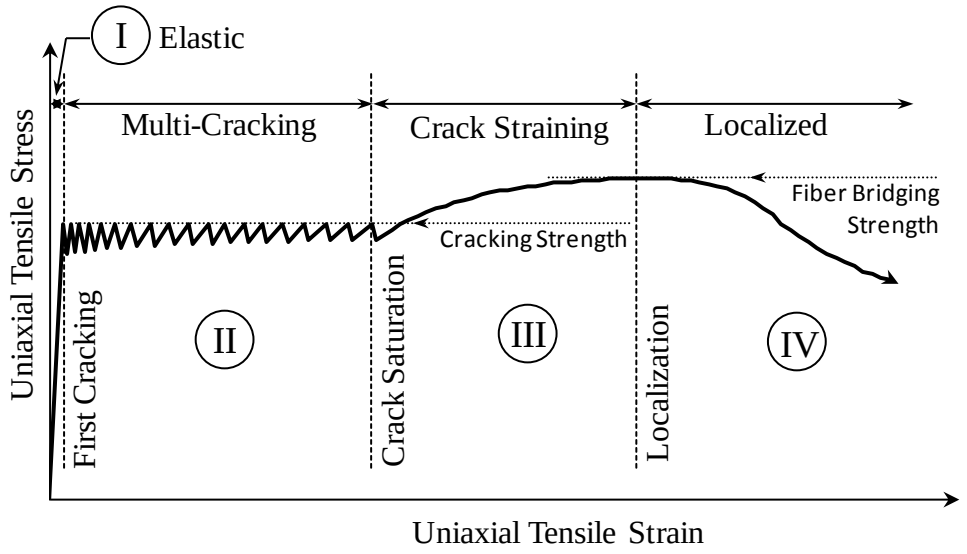

Figure 5. Graph. Idealized uniaxial tensile mechanical response of a UHPC

Standard tensile test methods designed to assess the cracking strength of conventional concrete may be appropriate for assessing the first cracking strength of UHPC, but are unlikely to be appropriate for quantitatively assessing the post-cracking tensile response of UHPC. The ASTM C78—Standard Test Method for Flexural Strength of Concrete (Using Simple Beam with Third-Point Loading) and ASTM C496—Standard Test Method for Splitting Tensile Strength of Cylindrical Concrete Specimens fall into this category. Both test methods include assumptions of mechanical behaviors that are not consistent with strain-hardening fiber-reinforced concretes and thus are likely to overestimate the tensile strength of the UHPC.

Graybeal has proposed a modified version of ASTM C496. The modified test method includes a requirement to monitor the first cracking of the UHPC during the test and calculate the splitting tensile strength based on the observed first cracking load.

Flexure-based test methods have been proposed, and in some cases, standardized. ASTM C1018 (withdrawn), ASTM C1609, and RILEM TC 162-TDF all present test methods for use in determining the tensile response of fiber-reinforced concretes. Methods have been proposed for analyzing the test results so as to develop uniaxial tensile response curves. However, these types of flexure tests have been demonstrated to be susceptible to overindications of strength as a result of the use of inappropriate support
conditions.

A variety of direct tension test methods have been developed. In a direct tension test, the UHPC specimen is loaded in uniaxial tension and thus the tensile response can be directly captured by measuring the load on and the strain experienced by the specimen. Direct tension tests can be divided into two groups, namely, tests that allow rotation of the ends of the test specimen and tests that do not. The tests with rotation might provide an indication of first cracking strength, but are not appropriate for assessment of post-cracking behaviors. This is because local inconsistencies in stiffness at the plane of the first crack result in rotation and fiber pullout at this

crack prior to the generation of a full set of additional cracks. Fixed-end tests that do not allow rotation at cracks are appropriate for capturing the full tensile stress-strain response. However, these tests are difficult to complete because of the bending stresses that can be imparted to the specimen during initial setup.

Graybeal reported measurements of tensile strength using flexural prisms, split cylinders, mortar briquettes, and direct tension tests of cylinders. The combined results of these tests indicated a first tensile cracking strength of approximately 1.3 ksi (9.0 MPa) for steam-cured specimens and approximately 0.9 ksi (6.2 MPa) without any heat treatment.

The modulus of rupture values for first cracking determined by the ASTM C1018 prism flexure test varied from 1.3 to 1.5 ksi (9.0 to 10.3 MPa), depending on the method of steam curing, and had an average value of 1.3 ksi (9.0 MPa) for untreated specimens. These specimens exhibited large deflections before the post-cracking peak load was reached.

In the split cylinder tests (ASTM C496), measured splitting tensile strengths at first cracking were 1.7 ksi (11.7 MPa) for steam-cured specimens and 1.3 ksi (9.0 MPa) for untreated specimens. For the steam-cured specimens, the splitting tensile strengths at first cracking varied from 3 to 5 percent of the measured compressive strength. The post-cracking peak tensile splitting stresses ranged from 12 to 16 percent of the compressive strength.

First cracking tensile strengths using briquettes in accordance with AASHTO T 132 ranged from 1.0 to 1.4 ksi (6.9 to 9.7 MPa), depending on the method of steam curing. For untreated specimens, the average value was 0.9 ksi (6.2 MPa).

In the direct tensile tests of 4- by 8-inch (102- by 203-mm) cylinders, first tensile cracking occurred between 1.1 and 1.6 ksi (7.6 and 11.0 MPa), depending on the method of steam curing, and between 0.8 and 1.0 ksi (5.5 and 6.9 MPa) for untreated specimens.

In this study, Graybeal concluded that the tensile strength (f_{ct}) of UHPC can be related to the measured compressive strength (f'_c) by the equation in figure 6.

$$f_{ct} = 7.8\sqrt{f'_c} \text{ or } 8.3\sqrt{f'_c} \text{ depending on the method of steam curing}$$

$$f_{ct} = 6.7\sqrt{f'_c} \text{ for untreated specimens}$$

Figure 6. Equation. Concrete tensile strength approximations

Subsequent research by Graybeal and Baby on this topic has resulted in the development of a uniaxial direct tension test method applicable to UHPC. This test method, whose concept is based on a standard tension test applied to metals, provides the uniaxial tensile mechanical response of UHPC and is applicable to both cast and extracted test specimens. Tests were completed on two UHPCs containing multiple steel fiber reinforcement percentages and cured through ambient laboratory and steam-treated conditions. The results demonstrated that these two UHPCs could sustain more than 1.3 ksi (9 MPa) of uniaxial tensile load through a strain of at least 4,000 millionths.

Baby, Graybeal, Marchand, and Toutlemonde investigated the use of flexural tensile test methods for UHPC and the associated analyses necessary for appropriate interpretation of the results. These analyses, often referred to as inverse analyses, derive the uniaxial tensile response from the observed load, deflection, and possibly surface strains observed during a flexure prism test. This research demonstrated that flexure test methods can be applied, but that capture of specific response observations are necessary and appropriate interpretation of data is critical. This research was conducted alongside the research presented in Graybeal and Baby, allowing direct comparison of results.

Reineck and Frettlöhr investigated the effect of specimen size on the flexural and axial tensile strengths. The depth of the flexural specimens ranged from 1 to 6 inches (25 to 150 mm) with width-to-depth ratios ranging from 1 to 5. The same sizes and ratios were used for the axial tension tests. The authors reported a decrease in both strengths with increasing size of the test specimens.

Schmidt and Fröhlich observed that specimens heat cured at 194°F (90 °C) for 48 hours and tested in flexure had a 15-percent higher flexural strength than specimens stored continuously at 60 °F (20 °C).

A study by Wille and Parra-Montesinos investigated the effects of beam size, casting method, and support conditions on UHPC flexure test results. The study reported that large discrepancies in results were possible for an individual UHPC, depending on the test setup and specimen characteristics.

MODULUS OF ELASTICITY

Graybeal measured the modulus of elasticity in compression in accordance with ASTM C469 at ages from 1 to 56 days for cylinders cured according to the four regimes described under Compressive Strength. Reported values were mostly the average value of six cylinders. After steam curing, the measured values were about 7,250 ksi (50 GPa). Cylinders cured under standard laboratory conditions had modulus of elasticity values of about 6,200 ksi (42.7 GPa) at 28 days. In terms of strength, modulus of elasticity, and strain at peak load, the UHPC showed very little change after completion of steam curing. The specimens cured under laboratory conditions continued to gain strength for at least 8 weeks after casting but the increase in modulus of elasticity and the decrease in strain at peak load seemed to stop at about 1 month.

The modulus of elasticity was also measured in direct tension tests. The average measured values were 7,500 ksi (51.9 GPa) for steam-treated specimens and 6,900 ksi (47.6 GPa) for untreated specimens. These values were slightly higher than measured in compression.

The equation in figure 7 or modulus of elasticity was proposed by Graybeal based on the general form of the AASHTO equation and values of f'_c between 4.0 and 28.0 ksi (28 to 193 GPa).

$$E_c = 46200\sqrt{f_c'} \quad \text{in psi units}$$

Figure 7. Equation. Graybeal equation for UHPC modulus of elasticity[22,103]

where: E_c = modulus of elasticity
f'_c = UHPC compressive strength

Subsequent research by Graybeal has developed additional results related to the modulus of elasticity of UHPC. These tests, completed on a UHPC specifically formulated for use as a field-cast material in connections between structural components, found that the equation in figure 8 is inappropriate for strengths between 14 and 26 ksi (97 and 179 MPa). This research also investigated the impact of curing temperature on compressive mechanical response development and found that the modulus of elasticity is related to the compressive strength and is largely independent of curing temperature.

$$E_c = 49000\sqrt{f_c'} \quad \text{in psi units}$$

Figure 8. Equation. Graybeal equation for UHPC modulus of elasticity

Ma et al. developed the equation in figure 9 for UHPC containing no coarse aggregates:

$$E_c = 525{,}000 \quad \frac{f_c'}{10}^{\frac{1}{3}}$$

Figure 9. Equation. Ma et al. equation for UHPC modulus of elasticity

Modulus of elasticity values have also been reported by others.

Diederichs and Mertzsch measured the stress-strain relationships at concrete temperatures ranging from 68 to 1,560 °F (20 to 850 °C). They observed a large reduction in both strength and modulus of elasticity at the higher testing temperatures. At the same time, the strain at peak stress increased at the higher temperatures. The same observations were made by Pimienta et al. for temperatures ranging from 68 to 1,110 °F (20 to 600 °C). However, some or all of the loss was recovered after the specimens cooled down.

POISSON'S RATIO

Table 7 lists values of Poisson's ratio determined by various researchers.

Table 7. Values of Poisson's ratio

Poisson's Ratio	Reference (First Author)
0.2	Simon
0.16	Joh
0.21	Ahlborn
0.19	Bonneau
0.18	Graybeal
0.18	Ozyildirim

FATIGUE BEHAVIOR

Ocel and Graybeal reported a fatigue test of an AASHTO Type II girder. The upper limit of the fatigue load was just below the static load levels that would cause flexural and shear cracking of the girder. The first cracks were observed after 0.64 million cycles at the intersection of the web and bottom flange in one shear span. After 1.405 million cycles, the same cracks were observed in the other shear span. Flexural cracks were noticed in the constant moment region after 1.888 million cycles. These were accompanied by a longitudinal crack in the bottom flange. Testing continued to 12 million cycles, during which the existing cracks continued to lengthen and additional cracks occurred, but there was no indication of fatigue degradation or change in the global behavior of the girder.

Prior to construction of a UHPC bridge in the city of Calgary, a 39-inch (1-m)-long transverse section was tested in flexural fatigue. The section was subjected to 1 million cycles between 20 and 80 percent of the design service load, 1 million cycles between the 20 and 80 percent of the observed first cracking load, and 1 million cycles between 20 and 80 percent of the failure load for companion sections that contained fiber-reinforced plastic reinforcing bars. Following the fatigue testing, the specimen was loaded to failure with the maximum load being greater than expected.

Prior to construction of a UHPC waffle-slab bridge deck in Wapello County, IA, tests were conducted on specimens representing a full-scale portion of the bridge. A single point load representing a wheel load was placed at two critical locations. No fatigue damage was noted after 1 million cycles of loading at each location.

Graybeal and Hartmann conducted flexural fatigue tests on 2-inch (51-mm)-square beams. In one set of tests, uncracked specimens were loaded to produce different stress ranges. Most specimens survived more than 6 million cycles of loading. In a second series of tests, the specimens were precracked and then tested in fatigue with loads cycling from 10 to 60 percent of the cracking load. One specimen failed after 9,950 cycles, while the other failed after 129,700 cycles. In these tests, some of the steel fiber reinforcement was observed to have fractured rather than pulling out of the UHPC matrix.

Schmidt et al. investigated the fatigue behavior of UHPC cylinders loaded in axial compression at various stress range levels. They observed that specimens with a ratio of stress range to

compressive strength of 0.45 survived 2 million load cycles without failure. The test specimens that survived the 2 million cycles of loading had only a slight decrease in compressive strength compared with specimens without any preceding load cycles.

Fatigue tests of UHPC specimens under various combinations of stress level and stress range by Fitik et al. showed a range of cycles to failure from 2.5 to more than 7.0 million cycles. They attributed the wide range to local faults, which initiated the failure process.

Uniaxial compression tests reported by Grünberg et al. and Lohaus and Elsmeier with a minimum stress limit of 5 percent of the static strength and varying upper stress level resulted in the number of cycles to failure ranging from about 2.5 to 7.1 million.

Behloul et al. conducted flexural fatigue tests on 4- by 4- by 16-inch (100- by 100- by 400-mm) prisms made of two different UHPC formulations. Prior to fatigue loading, the specimens were loaded to produce a crack opening of 0.012 inches (0.3 mm). The specimens were then cycled at 5 Hz between 10 and 90 percent of the first cracking strength. After 1 million cycles, the specimens were loaded statically, and the results were compared with specimens not subjected to fatigue loading. The fatigue loading appeared to have no effect on the overall mechanical behavior.

Lappa et al. reported flexural fatigue tests of 5- by 5- by 40-inch (125- by 125- by 1,000-mm) beams with a maximum load equal to about 75 percent of the static strength. The number of cycles to achieve fatigue fracture ranged from 29,295 to 170,771.

THERMAL PROPERTIES

Coefficient of Thermal Expansion

Coefficients of thermal expansion (COTE) measured by various researchers are shown in table 8.

Table 8. Values of coefficients of thermal expansion

COTE		Reference
Millionths/°F	**Millionths/°C**	**First Author**
8.2 to 8.7	14.7 to 15.6	Graybeal
6.7	12	Fehling
5.6 to 6.7	10 to 12	Simon
7.6 to 8.2	13.6 to 14.8	Ahlborn
6.7	12	Behloul

The French Interim Recommendations state a value of 6.1 x 10^{-6}/°F (11 x 10^{-6}/°C) if no other value can be determined.

Heat of Hydration

Graybeal measured heat of hydration in a well-insulated calorimeter and reported a temperature rise of about 65 °F (36 °C).

BOND STRENGTH

Carbonell et al. investigated the bond strength between conventional concrete substrates and UHPC toppings. Primary variables were surface temperature and moisture condition of the substrate. Half the specimens were subjected to 300 freeze-thaw cycles in accordance with ASTM C666 Method B. The authors evaluated bond strength using an indirect splitting tensile test along the interface. Samples subjected to the freeze-thaw tests had greater bond strength than samples of the same age without freeze-thaw cycles. Samples in which the substrate was saturated before placing the UHPC achieved higher bond strengths than samples with a dry substrate.

IMPACT RESISTANCE

Bindiganvile et al. compared the impact resistance of UHPC with that of conventional fiber reinforced concrete (FRC). Under quasistatic loading, UHPC was two to three times stronger in flexure and absorbed three times greater energy than conventional steel FRC or polypropylene FRC. Under impact loading, the UHPC was approximately twice as strong as conventional FRC and dissipated three to four times as much energy.

Cadoni et al. observed that the first cracking stress under dynamic loading was two to three times greater than under static load. The impact resistance of UHPC for use in piles was investigated by Leonhardt et al.

Further discussion of impact resistance can be found in chapter 6 under the discussion of security applications.

CREEP

The standard test method for creep in North America is ASTM C512. In this test, specimens are subjected to a constant axial stress, and the change in length over time is measured. Results may be expressed as a creep coefficient = creep strain/initial strain or specific creep = creep strain/ applied stress.

Graybeal conducted creep tests on 4-inch (102-mm)-diameter cylinders loaded at ages of 4, 21, and 28 days depending on the method of curing. Creep coefficients after 1 year ranged from 0.29 to 0.78, and specific creep ranged from 0.04 to 0.15 millionth/psi (5.7 to 21.2 millionths/ MPa), depending on the method of curing and loading age. For reference, the specific creep of conventional concrete is in the range of 0.25 to 1.0 millionths/psi.

Graybeal also conducted creep tests on 4-inch (102-mm) diameter cylinders with compressive strengths between 8.0 and 13.0 ksi (55 and 90 MPa) at stress-to-strength ratios ranging from 0.60 to 0.85 to represent the application of prestressing forces prior to steam curing. Measured creep

coefficients after 30 min under sustained load ranged from 0.32 to 0.85. These values would be considered high for the short duration of loading.

Burkhart and Müller measured the effect of age of loading, specimen size, stress level, and curing conditions (sealed and unsealed) on the creep of UHPC. Reported specific creep values after about 100 days under load ranged from 0.11 to 025 millionths/psi (16 to 35 millionths/MPa). Measured creep coefficients after 100 days under load were between about 0.9 and 1.3. The measured creep was observed to decrease with age at loading and increased specimen size. This behavior is similar to that of conventional concrete.

Ichinomiya et al. reported specific creep values ranging from 0.19 to 0.28 millionths/psi (28 to 40 millionths/MPa) after 150 days under load for specimens loaded at 2 and 4 days. For specimens loaded at 28 days, the specific creep was about 0.08 millionths/psi (11 millionths/MPa) after about 120 days.

Acker and Behloul reported specific creep values between 0.30 and 0.22 millionths/psi (43 and 32 millionths/MPa) for ages of loading between 4 and 28 days. Fehling et al. reported specific creep values between 0.32 and 0.15 millionths/psi (47 and 22 millionths/MPa) and creep coefficients between 2.27 and 1.08 for ages of loading between 1 and 28 days.

Francisco et al. reported creep strains of about 1,000 millionths after 30 days under load at a stress of about 8.7 ksi (60 MPa), corresponding to a specific creep of about 0.12 millionths/psi (17 millionths/MPa). The 2.75-inch (70-mm)-diameter cylinders were cured at 122 °F (50 °C) prior to loading at an age of 2 days. Drying creep was negligible.

Francisco et al. showed that the specific creep was about the same for heat-treated UHPC specimens loaded at an age of 2 days to 25 and 40 percent of the compressive strength. Flietstra et al. investigated the creep caused by applying a compressive stress and then subjecting the loaded specimens to different curing regimes. This test simulated transfer of the prestressing force prior to heat treatment.

SHRINKAGE

Two types of shrinkage may be present in UHPC. Drying shrinkage is that caused by loss of moisture from the UHPC. Autogenous shrinkage is that caused by a decrease in volume as the cementitious materials hydrate. The standard test in the United States for measuring shrinkage is ASTM C157, which is designed to measure drying shrinkage beginning after the concrete has hardened. Other methods are used to measure autogenous shrinkage because these measurements must begin immediately after the UHPC is placed.

Shrinkage of UHPC measured in accordance with ASTM C157 using 3- by 3-inch (76- by 76-mm) prisms provided an ultimate shrinkage range of 620 to 766 millionths, depending on the method of steam curing, and 555 millionths for untreated specimens. The initial shrinkage rate of UHPC was also measured in separate tests. During the initial hydration period, peak shrinkage of 64 millionths/hour was measured. As much as 400 millionths of shrinkage occurred in the first 24 hours for untreated specimens. Following steam curing, further shrinkage was almost eliminated.

Measurements of shrinkage by Burkhart and Müller starting 1 or 2 days after casting showed no difference between sealed and unsealed cylinders and among specimens with diameters of 3, 4, and 6 inches (75, 100, and 150 mm). They attributed most of the shortening to that caused by autogenous shrinkage, with very little caused by drying shrinkage. All values were about 300 millionths after 200 days of measurements. Autogenous shrinkage values of 600 to 900 millionths at 28 days were reported by Eppers and Müller, 200 to 550 millionths at 150 days by Ichinomiya et al., and about 640 millionths at 365 days by Lallemant-Gamboa et al.[135,92,93]

Fehling et al. reported total shrinkage of 700 and 900 millionths at 7 and 28 days, respectively, for sealed specimens. For specimens subjected to heat treatment, the subsequent shrinkage was negligible.

Francisco et al. reported autogenous shrinkage of about 270 millionths and drying shrinkage of about 100 millionths at 350 days on 2.75-inch (70-mm)-diameter cylinders cured at 122 °F (50 °C).

Ma et al. showed that the autogenous shrinkage could be reduced considerably by including a basalt coarse aggregate with an aggregate size ranging from 0.08 to 0.40 inches (2 to 5 mm). The coarse aggregate had a relatively small effect on the fresh concrete properties, compressive strength, and modulus of elasticity. Significant reduction of early age autogenous shrinkage was obtained by replacing silica fume with metakaolin in specimens cured at 68 °F (20 °C). For UHPC cured at 108 °F (42 °C), the total shrinkage measured for a mix containing metakaolin was negligible compared with mixes with silica fume or fly ash.

To offset the magnitude of autogenous shrinkage, Suzuki et al. and Kim et al. investigated the use of an expansive additive and a shrinkage reducing additive. Suzuki et al. reported that an autogenous shrinkage of more than 700 millionths would be reduced to zero with the use of these materials. Kim et al. reported that total shrinkage at 90 days was reduced from 800 to 400 millionths.

SUMMARY OF MECHANICAL PROPERTIES

The application of heat curing has a significant and immediate impact on the mechanical properties of UHPC. It increases the compressive strength, tensile cracking strength, and modulus of elasticity. It decreases creep and virtually eliminates subsequent shrinkage. These beneficial properties can also be achieved without heat curing. However, the effect is reduced, and it takes a longer time to achieve the beneficial properties.

Sufficient information has been published about the mechanical properties of UHPC to establish a range of properties to consider in structural design. These are listed in table 9.

Table 9. Range of UHPC material properties

Property	Range	
Compressive strength	20 to 30 ksi	140 to 200 MPa
Tensile cracking strength	0.9 to 1.5 ksi	6 to 10 MPa
Modulus of elasticity	6,000 to 10,000 ksi	40 to 70 GPa
Poisson's ratio	0.2	0.2
Coefficient of thermal expansion	5.5 to 8.5 millionths/°F	10 to 15 millionths/°C
Creep coefficient[1]	0.2 to 0.8	0.2 to 0.8
Specific creep[1]	0.04 to 0.30 millionths/psi	6 to 45 millionths/MPa
Total shrinkage[2]	Up to 900 millionths	Up to 900 millionths

[1] Depends on curing method and age of loading.
[2] Combination of drying shrinkage and autogenous shrinkage and depends on curing method.

Creep of UHPC is much less than conventional concrete. This results in reduced prestress losses but can be detrimental if relied on to reduce stresses in restrained members.

The total shrinkage reported in table 9 includes both drying and autogenous shrinkage. From the reported data, most of the shrinkage is autogenous shrinkage.

UHPC has sufficient fatigue resistance in both tension and compression to resist several million cycles of loading. Its impact strength is two to three times higher than its static strength.

CHAPTER 4. STRUCTURAL DESIGN AND STRUCTURAL TESTING

This chapter summarizes available information about the structural design of UHPC members and the testing that has been performed on structural members. The different sections in this chapter correspond to articles in the AASHTO Load & Resistance Factor (LRFD) Bridge Design Specifications.

As noted in chapter 3, it is important to recognize that the dispersion and orientation of the fiber reinforcement are critical parameters that influence the structural behavior of UHPC. The fiber reinforcement serves to resist tensile stresses in the UHPC component both before and after tensile cracking of the UHPC matrix. Post-cracking structural response of UHPC is particularly susceptible to degradation from disadvantageous fiber dispersion and/or orientation. Mixing and placing methods can affect the hardened UHPC mechanical response and thus must be appropriately coordinated to ensure acceptable structural performance. A framework for addressing the reliance on fiber reinforcement in the tensile mechanical resistance of UHPC structural components has been presented in the Service d'étude des transports, des routes et de leurs aménagement-Association Francaise de Genie Civil (SETRA-AFGC) design recommendations.

FLEXURAL AND AXIAL LOADS

Flexural Members

The calculated flexural resistance of concrete components is generally based on the conditions of equilibrium of forces and strain compatibility. The usable compressive strain in unconfined concrete is limited to a maximum value of 0.003. The shape of the stress-strain curve may be any shape that results in a prediction of strength in substantial agreement with test results. For simplification, a rectangular stress block for the compression zone is usually assumed. The tensile strength of the concrete is neglected. The applicability of this approach for use with UHPC has been addressed in several articles.

Graybeal tested a 36-inch (0.91-m)-deep AASHTO Type II girder made of UHPC in flexure using four-point bending on a span length of 78.5 ft (23.9 m).(See figure 10.) The girder contained twenty-four 0.5-inch (12.7-mm)-diameter strands. Prior to reaching peak load, the girder achieved a deflection of almost 19 inches (480 mm) and failed by a combination of tensile fracture of the strands and pullout of the fibers.

Figure 10. Photo. Flexural test of an AASHTO Type II girder made of UHPC

The peak applied load on the girder produced a bending moment of 38,700 kip-inches (4,370 kN-m). A flexural analysis, assuming a rectangular stress block and that the UHPC carried no tensile forces after cracking, produced a calculated moment capacity of 27,840 kip-inches (3,150 kN-m)—considerably less than the measured strength. Based on analysis of the measured data, Graybeal proposed that flexural capacity could be calculated more accurately assuming the following UHPC stress-strain curve:

- In compression, a linear relationship up to 0.85 times the compressive strength.
- In tension, a rigid-plastic relationship with a conservative value of post-cracking tensile strength and a limiting tensile strain.

For his test data, stress-strain relationships would be as follows:

- In compression, a linear relationship from the origin to a compressive stress of 24 ksi (165 MPa). Based on the graphical depiction, the modulus of elasticity appears to be about 8,000 ksi (55 MPa).
- In tension, a constant stress of 1.5 ksi (10.3 MPa) over a strain range from zero to 0.007.

The flexural strength of the section can then be calculated using a traditional mechanics of materials approach.

Graybeal also tested two pi-girders made of UHPC in flexure using four-point bending. The span lengths of the girders were 69 and 45 ft (21 and 13.72 m). The girders achieved deflections of about 10 and 5 inches (250 and 125 mm) before reaching a peak load. The failure mechanisms of the two girders were similar. The fibers began to pull out from the matrix at a crack near midspan. This shed the tensile force from the fibers to the prestressing strands, which then fractured. The moments at first flexural cracking of the girders were 20,600 and 19,500 kip-inches (2,330 and 2,200 kN-m). The ultimate flexural capacities of the girders were

37,600 and 38,190 kip-inches (4,250 and 4,310 kN-m). A third girder that was intended to fail in shear failed in flexure at a moment of 36,720 kip-inches (4,150 kN-m). Based on an analysis in accordance with the AASHTO LRFD Bridge Design Specifications, a 70-ft (21.3-m) girder has a Service III moment demand of 19,940 kip-inches (2,250 kN-m) and Strength I moment demand of 39,600 kip-inches (4,470 kN-m). The cracking moments observed in the experiment were approximately equal to the Service III moment. The measured flexural capacities were, on average, about 5 percent less than the required values, indicating the need for additional flexural reinforcement.

Meade and Graybeal reported the results of sixteen 6-inch (152-mm)-wide, 15-inch (381-mm)-deep rectangular UHPC beams tested in four-point bending over a span length of 16 ft (4.88 m). The test variables were fiber content (0, 1, and 2 percent by volume) and quantity of conventional nonprestressed reinforcement (0.00 to 1.00 percent by area). Measured compressive strengths of the UHPC ranged from 24.7 to 29.4 ksi (170 to 203 MPa).

Beams containing 1- and 2-percent fiber reinforcement had higher first cracking strengths, better post-cracking flexural response, and higher peak loads than beams without fibers. Increasing the fiber content from 1 to 2 percent resulted in stiffer post-cracking response and higher peak loads. The beams containing no fibers failed when flexure-shear cracks extended into the compression region under the load points, leading to a shear failure of the flexural compression block in the shear span. The beams containing the fibers failed when the fibers pulled out across a critical crack and the reinforcing bars ruptured. No concrete crushing was noted.

Visage et al. reported the results of ten 6-inch (152-mm)-square beams tested in flexure. Test variables included compressive strength, amount of flexural reinforcement, volume of steel fibers, and beam length. Test results were compared with traditional methods of estimating moment-curvature relationships. Other flexural tests have been reported by Gröger et al., Frettlöhr et al., and Stürwald and Fehling.

Adeline and Behloul reported flexural tests of two 49.2-ft (15-m)-long UHPC beams containing only flexural reinforcement. The beams contained eight or four 0.6-inch (15.2-mm)-diameter strands. The beam with eight strands failed by crushing of the UHPC, whereas the beam with two strands failed by strand rupture. Both beams exhibited large deflections before failure. The authors used a nonlinear multilayer program to predict the moment-deflection curves. They obtained very good agreement between the measured and calculated curves in both the elastic and plastic parts of the curves.

Maguire et al. tested two full-size double-tee beams in flexure. The beams contained 0.7-inch (17.8 mm)-diameter strands and UHPC without steel fibers. The measured strengths exceeded the calculated strengths using measured properties and a strength design approach. The authors concluded that the flexural design procedures of the AASHTO LRFD Specifications for I-girders are applicable to UHPC girders.

Steinberg and Reeves examined the reliability of the flexural strength of UHPC AASHTO standard box beams based on the AASHTO LRFD Bridge Design Specifications. The reliability analysis consisted of a Monte Carlo simulation and the use of the moment-curvature

approach to calculate flexural strength. The authors concluded that the use of the AASHTO LRFD Specifications produces a conservative reliability index when applied to UHPC members. For lightly reinforced members, the design may be overly conservative. To rectify this, they suggested using a more advanced analysis method, such as moment-curvature, or increasing the strength reduction factor.

Prior to construction of Malaysia's first UHPC motorway bridge, a prototype I-girder was tested in flexure using a single point load at midspan. The load-deflection curve predicted by finite element modeling matched the measured values very closely.

Sujivorakul developed a flexural model to predict the moment-curvature relationship for doubly reinforced UHPC beams. The model is based on strain compatibility, equilibrium of forces, and the stress-strain relationship of UHPC in tension and compression.

For strength design, Stürwald and Fehling developed a simplified approach. They used a triangular stress block in compression and a rectangular stress block for tension in the UHPC. This approach gave calculated strengths within 5 percent of the measured strength of three beams.

Moment Redistribution

Walsh and Steinberg examined the moment redistribution capacity of four small-scale continuous two-span UHPC beams with no conventional reinforcement. The test results suggested that the moment redistribution of UHPC is comparable to the 20-percent maximum given in the AASHTO LRFD Bridge Design Specifications.

Compression Members

Tue et al. examined the capacity of stub columns of UHPC confined by a steel tube. The load was applied either to the combined steel and UHPC section or to the UHPC section alone. The authors observed that shrinkage of the UHPC produced a gap between the UHPC and the inside of the steel tube. This gap only closed after the stresses exceeded the service level and lateral strains increased considerably. As such, the confinement effect was not as effective as that achieved with conventional concrete.

Empelmann et al. tested six short columns in concentric compression. The 7.9- by 7.9- by 23.6-inch (200- by 200- by 600-mm) columns contained different amounts of longitudinal and transverse reinforcement.

Yan and Feng also tested short UHPC columns with a diameter of 4.3 inches (110 mm) inside steel tubes with a wall thickness of 0.19 to 0.26 inches (5 to 6.5 mm). Measured compressive strengths were greater than calculated by the equation in figure 11.

$$N = f_y A_s + f_c' A_c$$

Figure 11. Equation. Strength of columns

where:
f_y = tensile yield strength of the steel tube
A_s = cross sectional area of the steel tube
f'_c = compressive strength of 4-inch (100-mm) UHPC cubes
A_c = cross sectional area of the concrete

The authors noted that confinement of the steel tube was not as effective as that for conventional concrete, and therefore, the effect can be neglected in the calculation of axial load.

Tension Members

A method for measuring the uniaxial tensile stress-strain response has recently been developed by a U.S.–French joint project. The test method provides the response for both precracking and post-cracking phases without requiring any complex stress or strain transformations.

Jungwirth and Muttoni reported the results of direct tension tests on dog-bone shaped specimens having a test cross section of 1.8 by 6.3 inches (45 by 160 mm). They reported a linear stress-strain relationship with a modulus of elasticity of about 8,700 ksi (60 GPa) up to a tensile stress of 1.2 ksi (8.5 MPa). Following cracking of the specimens, the tensile stress increased to about 1.45 ksi (10 MPa) before the fibers progressively pulled out at a strain of about 2.5 percent. The authors also performed tests on specimens containing nonprestressed reinforcement ranging from 1 to 4.5 percent by area. All specimens exhibited well-distributed cracking and strains as high as 10 percent.

Further discussion of the tensile response of UHPC is provided in chapter 3 under the heading of tensile strength.

Bearing

Holschemacher et al. investigated the bearing strength of two UHPCs, with and without helical reinforcement, using two different specimen heights and different diameters of loading area. Results were compared with the German Standard DIN 1045-1. The results indicated that the strengths calculated using DIN 1045-01 equations need to be modified by a factor such as 0.8 for them to be applicable to UHPC.

Hegger et al. tested various details for joints between precast UHPC columns. The major test variables included dry and wet joints. With dry joints, the surface treatment of the interface surfaces and the longitudinal reinforcement ratio were variables. With wet joints, the mortar thickness and transverse reinforcement ratios with welded wire reinforcement and steel plates were variables. Measured bearing capacities were slightly less than measured on a continuous reference column.

SHEAR AND TORSION

Sectional Design

The AASHTO LRFD shear design sectional model involves the calculation of three components that contribute to shear resistance. They are the concrete contribution, the transverse or shear reinforcement contribution, and any vertical component of prestressing force from draped strands. The procedure involves a combination of theory and empirical factors. In UHPC beams with no conventional transverse reinforcement, there is no reinforcement contribution. The tensile stresses that develop are carried by the UHPC matrix and steel fibers.

Graybeal tested three 36-inch (0.91-m)-deep AASHTO Type II prestressed UHPC girders in shear. The girders contained no nonprestressed shear reinforcement. Each girder failed in a different manner. The first girder failed owing to a preexisting horizontal crack at the base of the web from a prior flexural test. The second girder failed owing to diagonal tension in the shear region. The third girder failed owing to a combination of diagonal tension and strand slip. Because the girders did not contain any nonprestressed shear reinforcement and no draped strands, Graybeal proposed that the shear capacity could be determined by assuming that all the shear forces are carried by diagonal tension and compression in the web of the girder. The limiting value is the post-cracking tensile strength of the UHPC. A conservative estimate of this value would be required. In addition, it is necessary to determine the state of stress in the girder under dead load and prestressing forces.

Graybeal also tested three 33-inch (838-mm)-deep pi-girders with shear spans of 7.0, 6.0, and 6.0 ft (2.13, 1.83, and 1.83 m) under three-point bending. First, shear cracks appeared at shear loads of 175, 180, and 205 kips (780, 800, and 910 kN). The shear loads at failure were 430, 366, and 510 kips (1,910, 1,630, and 2270 kN). However, the third girder failed in flexure rather than loss of diagonal tensile capacity in the web as occurred in the first two girders. Based on an analysis in accordance with the AASHTO LRFD Bridge Design Specifications, a 70-ft (21.3-m)-span girder has a Service III shear demand of 103.2 kips (459 kN) and a Strength I shear demand of 206 kips (916 kN).[76] The measured shear strengths were at least 75 percent greater than the Strength I demand. Based on the assumption that the girder webs carried all the shear force and that the diagonal tensile force acted uniformly over the relevant cross-sectional area of the webs, the calculated diagonal tensile capacities corresponding to the shear loads at failure were 2.5, 2.1, and 2.9 ksi (17.2, 14.6, and 20.3 MPa) for the three girders.

Maguire et al. reported shear tests of two full-size double-tee beams. The beams contained vertical shear reinforcement consisting of welded wire reinforcement with cross wires for anchorage. The UHPC did not contain any steel fibers. Both girders had a measured shear strength that exceeded the calculated shear strength based on measured material properties. The authors concluded that the AASHTO LRFD Bridge Design Specifications for shear design of I-girders is applicable to UHPC girders.

Baby et al. reported on a study investigating the shear performance of UHPC beams. Study variables included prestressed versus nonprestressed beams, the inclusion of stirrups for shear reinforcement, and the inclusion of fiber reinforcement. Supplemental beams were cast and

then deconstructed to extract prismatic specimens from the web region for three-point bending tests. These small-scale tests provided an indication of the fiber reinforcement orientation and effectiveness as shear reinforcement in the web. This research found that the shear design recommendations contained within the SETRA-AFGC UHPFRC Design Guidelines were conservative for these beams.

Shear tests of UHPC beams without conventional shear reinforcement were conducted by Bunje and Fehling.[165] All specimens failed in flexure. Other shear tests were conducted by Hegger et al., Hegger and Bertram, Cauberg et al., Fehling and Thiemicke, and Bertram and Hegger.

Hegger and Bertram tested 15.7-inch (400-mm)-deep prestressed concrete I-beams with a length of 185 inches (4.70 m). Four series of beams were tested as follows:

- Beams without openings (11 tests).
- Beams with a single web opening (9 tests).
- Beams with several web openings (7 tests).
- Beams with additional shear reinforcement near the openings (9 tests).

The beams in the first three series did not contain any conventional transverse reinforcement.

For beams without openings, the shear strength increased as the fiber content increased. An increase in the prestressing force resulted in an increase in the shear strength. The provision of a single opening reduced the shear strength. However, the strengths of beams with two openings were similar to those of beams with a single opening.

Wu and Han reported tests of 11 reinforced concrete I-girders of which 8 failed in shear. The main variables were fiber volume content, flexural reinforcing steel ratio, section type, and span/depth ratio. No shear reinforcement was provided in the webs. Based on the test results, a formula for the first diagonal cracking load was developed. The authors concluded that the conventional equations for calculating shear strength are not appropriate and developed an analytical model.

Prior to construction of Malaysia's first UHPC motorway bridge, a prototype I-girder was tested in shear using a single point load at midspan. No conventional shear reinforcement was included. The shear strength predicted by finite element modeling was 17 percent lower than the measured strength.

Punching Shear

Section 9 of the AASHTO LRFD Bridge Design Specifications requires a minimum deck thickness of 7.0 inches (175 mm) unless approved otherwise by the owner. This generally precludes the likelihood of a punching shear failure in a bridge deck. The use of thinner sections with UHPC increases the likelihood of a punching shear failure and, therefore, the need to consider it in design.

Harris and Roberts-Wollmann tested twelve 45-inch (1,140-mm)-square UHPC slabs in punching shear. The variables in the program were slab thicknesses of 2.0, 2.5, and 3.0 inches (51, 64, and 76 mm) and loading plate dimensions from 1.0 to 3.0 inches (25 to 76 mm) square. No conventional reinforcement was included. The measured compressive strength of the UHPC was 32.1 ksi (221 MPa). Seven of the specimens failed in punching shear and five in flexure. The authors concluded that the American Concrete Institute (ACI) 318 equation for punching shear predicted the failure loads reasonably well but a modified version of the ACI model for breakout loads provided the best prediction. They also concluded that a 1.0-inch (25-mm) slab thickness should provide sufficient thickness to resist punching shear in bridge deck applications.

Three larger slabs with dimensions of 7.0 by 12.0 ft and 3 inches thick (2.1 by 3.7 m by 76 mm) were loaded with a wheel patch load. These tests represented the top flange of a double-tee section. The slabs all failed in tension.

Toutlemonde et al. investigated the local bending and punching shear performance of two-way ribbed bridge deck elements. Developed as a potential alternate for orthotropic bridge decks, these 15-inch (0.38-m)-deep deck elements were composed of a 2-inch (0.05-m)-thick plate and 13-inch (0.33-m)-tall bi-directional ribs with a 24-inch (0.6-m) center-to-center spacing. This study tested two different commercially available UHPC products. The punching shear capacity of the deck plate was observed to be greater than 157 kips (700 kN) under all conventional loading scenarios. When the wheel patch was reduced to a 7.5 x 10.2 inch (0.19 x 0.26 m) size, the authors observed the punching shear resistance to be between 79 and 94 kips (350 and 420 kN).

Naaman et al. evaluated the effect of fibers on the punching shear response of 7-inch (175-mm)-thick concrete bridge decks with and without reinforcing bars. Three different types of fibers were included. Test results showed that the punching shear resistance, the energy-absorption capacity, and the resistance to spalling of slabs having only two bottom layers of reinforcing bars were significantly better than for the control specimen with four layers of reinforcing bars and conventional concrete. The authors concluded that punching shear resistance can be safely taken as twice that calculated using the procedures of ACI 318-05.

Saleem et al. tested eight single-tee, simple span beams with a depth of 5 inches (125 mm), a top flange width of 12 inches (300 mm), and a span length of 48 inches (1219 mm). A center point load was applied over an area 19.7 inches (500 mm) long by 9.8 inches (250 mm) wide, representing an AASHTO HS20 truck dual tire wheel. All beams contained longitudinal flexural reinforcement but only two beams had shear reinforcement. The dominant mode of failure in the beams was shear.

Aaleti et al. reported punching shear tests on the 8-inch (200-mm)-deep waffle slab system proposed for use on a bridge deck in Iowa. They concluded that the system would not experience punching shear failure under the traditional 10 by 20 inch (254 by 508 mm) wheel loads. The measured punching shear strength was nearly 2.3 times the estimated value using the ACI equation recommended by Harris and Roberts-Wollmann.

Punching shear tests were reported by Joh et al. Tests were made on 63-inch (1,600-mm)-square slabs with thicknesses of 1.6 and 2.8 inches (40 and 70 mm) and loaded through plates with dimensions of 2.0 by 2.0, 3.0, 3.9, or 4.9 inches (50 by 50, 75, 100, or 125 mm). The 1.6-inch (40-mm)-thick slabs reached their flexural strength before punching occurred. The 2.8-inch (70-mm)-thick slabs failed by typical punching at the center of the slab. The authors confirmed that the ACI 318 equation for punching shear gave a reasonable estimate of the strength.

Bunje and Fehling conducted punching shear tests of UHPC slabs with thicknesses of 1.2, 1.6, 2.0, and 3.1 inches (30, 40, 50, and 80 mm). The slabs did not appear to contain any conventional flexural reinforcement. All slabs failed in a ductile flexural mode with no punching failure.

Moreillon et al. reported punching shear tests in which the primary variables were slab thickness, reinforcement ratio, and fiber volume. The authors developed a model for predicting the punching shear strength.

Interface Shear

Twenty-four push-off tests were conducted by Banta to determine whether the horizontal shear design equations of the AASHTO LRFD Bridge Design Specifications accurately predict the horizontal shear strength between UHPC and lightweight concrete. The test variables were interface surface characteristics, interface area, and area of reinforcement crossing the interface. The author compared the test results of 19 specimens with a smooth interface with the equations in the 2004 version of the Specifications, assuming a resistance factor of 1.0 and a friction factor of 1.0. Calculated strengths were always greater than measured strengths. It should be noted that the cohesion and friction factors have been revised since publication of the 2004 version of the LRFD Specifications.

Maguire et al. cautioned that the contribution of the contact surface between precast UHPC girders and a cast-in-place conventional concrete deck should be ignored because of the difficulty of roughening the top surface of the UHPC girders.

Crane and Kahn investigated the interface shear capacity of five reinforced tee beams with UHPC for the web and high-performance concrete (HPC) for the top flange. Test variables included interface roughness and amount of interface shear reinforcement. Test results were compared with the shear friction equations of the AASHTO LRFD Bridge Design Specifications. The equations were unconservative in predicting the shear strength of smooth interfaces even with relatively high amounts of shear reinforcement. Consequently, it was recommended that a fluted interface be used.

Hegger et al. conducted direct shear tests on joints between precast elements subjected to various levels of compression. They included dry and wet joints with various types of contact surfaces.

Shear Connections

Graybeal evaluated the use of UHPC in shear connectors between precast deck panels and concrete or steel beams. He tested two full-size beam specimens. The first specimen included frequently implemented details used to connect precast concrete slabs to beams. Conventional grout was used. The second specimen used simplified connection details in combination with UHPC. The tested UHPC connections eliminated all interference points between the girder and deck connectors by engaging the mechanical strength of the UHPC to carry the loads between the connectors across an otherwise unreinforced plane. Each specimen was subjected to more than 11 million cycles of loading followed by a static test to failure. The applied loads surpassed the design loads required by the AASHTO LRFD Bridge Design Specifications. The author observed no damage in the UHPC connections after they were subjected to 168 psi (1.16 MPa) of cyclic horizontal shear stress and 789 psi (5.44 MPa) of static horizontal shear stress along the minimum shear plane.

Hegger et al. have tested headed stud and continuous shear connectors using push-off tests and a beam test. The test parameters for the continuous connector push-off tests were steel fiber content, transverse reinforcement ratio, and thickness of the connector. The amount of steel fibers had a minor effect on the connector strength if a minimum fiber ratio was maintained. The arrangement of transverse reinforcement influenced the connector strength, whereas the thickness of the connector influenced strength and the mode of failure. In the beam test, the plastic moment was developed with no cracks developing at the connector.

Jungwirth et al. and Kohlmeyer et al. also conducted push-off tests of continuous shear connectors.

Torsion

Fehling and Ismail tested 7-inch (180-mm)-square beams in pure torsion. The parameters included steel fiber type, steel fiber volume, longitudinal reinforcement ratio, and web reinforcement ratio. The use of longitudinal and transverse reinforcement in combination with the steel fibers provided the biggest increase in ultimate torsion capacity and ductility.

Joh tested three 12-inch (300-mm)-square beams in pure torsion. One beam contained no conventional reinforcement, one beam contained longitudinal reinforcement in the corners, and the third beam contained both longitudinal and transverse reinforcement. The cracking torque and torsional strength were reasonably predicted using thin-walled tube theory modified to account for the tensile strength of the UHPC.

Empelmann and Oettel conducted tests on seven 20-inch (500-mm)-square hollow boxes with a wall thickness of 2 inches (50 mm) at midlength. Test variables included fiber content, longitudinal reinforcement ratio, and transverse reinforcement ratio. Four specimens were loaded in pure torsion. Three specimens were loaded with a combination of torsion and axial force. The experimental results were compared with design equations for conventional concrete members based on a space truss model.

PRESTRESSING

Stress Limits

No recommendations about stress limits to be used in UHPC prestressed concrete members were identified. However, Graybeal reported high creep on cylinders loaded to between 60 and 92 percent of the compressive strength at compressive strength levels between 8.5 and 12.5 ksi (59 and 86 MPa).

Loss of Prestress

Loss of prestressing force includes an instantaneous loss when the strands are released and a time-dependent loss caused by creep and shrinkage of the concrete and relaxation of the prestressing strands. A reasonable estimate of the instantaneous loss can be made if the modulus of elasticity of the UHPC is known accurately. The AASHTO LRFD specifications provides two methods for predicting time-dependent losses:

- Approximate estimate of time-dependent losses.
- Refined estimate of time-dependent losses.

Both estimates rely heavily on empirical methods. The applicability of these methods for use with UHPC needs to be verified because this study identified no direct methods to measure prestress losses in UHPC.

Calculated prestress losses for Type II AASHTO girder based on material property tests were 35.6 ksi (245 MPa). This included 15.4 ksi (106 MPa) for instantaneous loss, 10.0 ksi (69 MPa) for shrinkage, 6.9 ksi (48 MPa) for creep, and 3.1 ksi (21 MPa) for relaxation.

REINFORCEMENT DETAILS

Article 5.10 of the AASHTO LRFD Bridge Design Specifications addresses reinforcement details. No specific publications addressing these details for use with UHPC were identified. It is likely, however, that most of these provisions could be used with UHPC because of UHPC's higher compressive and tensile strengths.

DEVELOPMENT AND SPLICES OF REINFORCEMENT

Deformed Bars in Tension

New York State Department of Transportation performed pullout tests of No. 4, 5, and 6 bars embedded 2.9, 3.9, and 4.9 inches (75, 100, and 125 mm), respectively, in 15.7-inch (400-mm)-diameter UHPC cylinders, which resulted in reinforcement fracture within the length of bar not cast into the UHPC.

Graybeal and Swenty conducted pullout tests on No. 4 reinforcing bars embedded into 6-inch (152-mm) cubes of two different UHPCs. The rebar was bonded to the field-cast UHPC for 3 inches only, with the remainder of the length debonded by a foam bond-breaker. All of the

specimens were cast and cured in ambient laboratory conditions. Pullout tests on a UHPC formulation intended for use in precast concrete applications resulted in pullout of the bar after the tensile yield strength of the bar had been surpassed. Pullout tests on a UHPC formulation intended for field-cast applications resulted in tensile rupture of the reinforcement.

Pullout tests were also performed by Holschemacher et al. using 0.32- and 0.39-inch (8- and 10-mm)-diameter bars. They observed that the bond strength and stiffness increased with testing ages. Fehling et al. also performed pullout tests on 0.47-inch (12-mm)-diameter bars with various amounts of concrete cover and embedment lengths.

Hossain et al. completed pullout and development length tests of glass fiber reinforced polymer (GFRP) rebar embedded in two different UHPC formulations. Both No. 5 and 6 bars were tested with both high and low modulus of elasticity GFRP formulations. Larger bars and longer bond lengths were observed to result in lesser bond strengths, with all specimens failing via bar pullout.

Deformed Bars in Compression

No publications about the development length of deformed bars in compression in UHPC were identified.

Lap Splices

Graybeal evaluated the performance of six connection details for use between precast concrete elements. Four connections represented transverse joints between full-depth precast concrete deck panels. Two connections represented longitudinal joints between adjacent deck bulb-tee girders. Table 10 provides the reinforcement details used in the connection regions. Bars from adjacent panels were offset by half the bar spacing.

Table 10. Reinforcement used in connections

Orientation	Bar Size	Bar Type	Lap Length, inches	Bar Spacing, inches	
				Top	Bottom
Transverse	No. 5	Headed uncoated	3.5	17.7	7.1
Transverse	No. 4	Hairpin epoxy coated	3.9	4.3	4.3
Transverse	No. 5	Straight galvanized	5.9	17.7	7.1
Transverse	No. 5	Straight uncoated	5.9	17.7	7.1
Longitudinal	No. 5	Headed uncoated	3.5	17.7	7.1
Longitudinal	No. 5	Straight uncoated	5.9	17.7	7.1

1 inch = 25.4 mm

The specimens were loaded on a simple span, with the load applied through a simulated wheel patch placed adjacent to the connection near midspan. Cyclic loads were applied first, with the test program including at least 2 million cycles to a load just below the cracking strength of the specimen followed by at least 5 million cycles to a load larger than the cracking strength of the

specimen. After the completion of the cyclic testing, each test specimen was statically loaded to failure. All the specimens survived 7 million cycles of fatigue loading.

The tests showed that noncontact, lap-spliced reinforcement in the transverse and longitudinal connections was not susceptible to debonding under cyclic and static loads. The development length of straight, uncoated No. 5 reinforcing bars in this test program was demonstrated to be equal to or less than 5.9 inches (150 mm) in a non-contact lap splice configuration.

Hegger et al. reported on direct tension tests of lap-spliced specimens. The test variables were bar diameter, lap length, steel fiber ratio, transverse reinforcement ratio, and concrete cover.

Hossain et al. reported on testing lap-spliced GFRP rebar in field-cast connections between prefabricated bridge deck elements. This testing, which included both static and cyclic flexural loading of the beam splice connections, demonstrated that 5.9- to 8.9-inch (150- to 225-mm) lap splice lengths can be appropriate for GFRP rebar embedded in UHPC.

Standard Hooks in Tension

No publications about the development length of standard hooks in tension in UHPC were identified. However, it is likely that the existing provisions of the AASHTO LRFD Bridge Design Specifications are applicable because of UHPC's higher compressive and tensile strengths.

Welded Wire Reinforcement

No publications about the development length of welded wire reinforcement in UHPC were identified. However, it is likely that the existing provisions of the AASHTO LRFD Bridge Design Specifications are applicable because of UHPC's higher compressive and tensile strengths.

Shear Reinforcement

No publications about the development length of shear reinforcement in UHPC were identified. However, it is likely that the existing provisions of the AASHTO LRFD Bridge Design Specifications are applicable because of UHPC's higher compressive and tensile strengths.

Development of Prestressing Strand

Measured transfer and development lengths from various researchers are summarized in table 11.

Table 11. Measured transfer and development lengths

Strand Diameter		Transfer Length		Development Length		Source
inches	mm	inches	mm	inches	mm	
0.6	15.2	14	356	< 35	< 890	Ruiz et al.
0.5	12.7	8.7 to 11.0	220 to 280	—	—	Bertram and Hegger
0.7	17.8	17 to 21	430 to 530	—	—	Maguire et al.
0.5	12.7	—	—	< 37	< 940	Graybeal

— No data reported.

Graybeal reported results of a study investigating the lap-splice length of unstressed prestressing strands. Strands were lapped inside UHPC prisms and then loaded in direct tension. Strand rupture failures indicated that that lap length for 0.5-inch (12.7-mm)-diameter strands is approximately 18 inches (457 mm), and the lap length for 0.6-inch (15.2-mm)-diameter strands is approximately 26 inches (660 mm).

Steinberg and Lubbers reported the results of pullout tests of 0.5-inch (12.7-mm)-diameter standard and oversize prestressing strands embedded 12, 18, and 24 inches (305, 457, and 610 mm) in UHPC. In comparison with conventional concrete having compressive strengths less than 4.0 ksi (28 MPa), the UHPC had higher bond strengths. The results indicated that the strand strength was developed in less than 12 inches (25.4 mm).

Based on tests with 0.5-inch (12.7-mm)-diameter seven-wire strands, Hegger et al. showed that the minimum cover and minimum clear spacing to prevent splitting in UHPC could be reduced to 1.5*d* and 2.0*d* where *d* is the strand diameter. This is less than required by the German DIN 1045-01 for conventional concrete. In other tests, a concrete cover less than 2.5*d* led to splitting cracks. The authors recommended a minimum cover of 2.5*d* and a minimum clear spacing of 2.0*d*.

STRUCTURAL ANALYSIS

Chen and Graybeal reported the results of a research program to develop finite element analysis modeling techniques applicable to UHPC structural components. The mechanical properties used in the modeling are given in table 12.

Results of the analysis using the values given in table 12 compared favorably with values measured during tests on an I-girder and a pi-girder.

Table 12. UHPC properties used in finite element modeling

	Value	
Property	**English Units**	**Metric Units**
Unit Weight	160 lb/ft^2	2,565 kg/m^2
Compressive Strength	29 ksi	200 MPa
Modulus of Elasticity	7,650 to 8,000 ksi	53 to 55 GPa
Poisson's Ratio	0.18	0.18
Post-Cracking Tensile Strength	1.4 to 2.3 ksi	9.7 to 15.9 MPa
Ultimate Tensile Strain	0.007 to 0.010	0.007 to 0.010

DESIGN GUIDELINES

The literature search identified the following national recommendations for UHPC:

- Design Guidelines for Ductal Prestressed Concrete Beams (Australia).
- Recommendations for Design and Construction of Ultra High Strength Fiber Reinforced Concrete Structures by the Japan Society of Civil Engineers.
- Ultra High Performance Fibre-Reinforced Concretes, Interim Recommendations prepared by AFGC (French Association of Civil Engineers) and SETRA (French Road and Traffic Government Agency (SETRA-AFGC 2002).

On a more global scale, the Fédération Internationale du Béton (*fib*) Task Group 8.6 is developing recommendations tailored to the design of UHPC structures. The table of contents of the draft version have been published in Walraven.

Design Guidelines in Australia

The Australian guidelines were developed for the design of prestressed concrete beams manufactured using Ductal®. Where possible, a limit state approach consistent with the design requirements of the Australian Standard for Concrete Structures AS3600-1994 was adopted. The design procedures are based on the principles of structural mechanics and the material properties and behavior reported in the literature. Design guidelines are provided for strength, serviceability, and durability.

The material design properties address behavior in compression and tension, modulus of elasticity, density, Poisson's ratio, creep, and shrinkage. Design guidelines are provided for strength in flexure, strength in shear, strength in torsion, flexural crack control at service loads, deflection at service loads, loss of prestress, and anchorage zones.

Theoretical flexural capacity is based on equilibrium of forces and strain compatibility using idealized stress-strain curves in compression and tension for UHPC. A strength reduction factor of 0.8 is used for sections containing bonded reinforcement and 0.7 for sections containing no

bonded reinforcement. Ductility is provided by limiting the ratio of neutral axis depth to effective depth to a maximum value of 0.4.

Shear strength of the UHPC in beams is based on limiting the principal tensile stress at the centroidal axis or at the junction of the web and flange to a maximum value based on a section uncracked in flexure. This maximum value is provided in figure 12. When beams contain stirrups or inclined tendons, their contribution to shear resistance may be included in the same way as conventional reinforced concrete design. An equation is provided for the punching shear strength.

$$5.0 + 0.13 \sqrt{f'_c} \text{ in SI units}$$

Figure 12. Equation. Shear strength of UHPC beams[(210)]

The torsional strength, for a member not containing torsional reinforcement, is taken as the pure torsion required to cause first cracking.

Flexural cracking is controlled by limiting the maximum tensile stress to 870 psi (6.0 MPa) in nonprestressed elements and 1,160 psi (8.0 MPa) in prestressed elements.

Short-term deflections are calculated using conventional procedures for uncracked sections and integration of curvatures for cracked sections. Long-term deflection calculations are based on an age-adjusted effective modulus.

The guidelines suggest that a reliable estimate of prestress losses can be obtained using the age-adjusted effective modulus.

The transfer length of prestressing strands is to be taken between $20d_b$ and $40d_b$ depending on the stress condition being analyzed, where d_b is the strand diameter.

Appendices to the guidelines provide design examples.

This document could provide a template for a similar set of guidelines based on the AASHTO LRFD Bridge Design Specifications.[(76)]

Design Document from Japan Society of Civil Engineers

The draft recommendations in Recommendations for Design and Construction of Ultra High Strength Fiber Reinforced Concrete Structures (Draft), published by the Japan Society of Civil Engineers in 2006, provide basic principles for design and construction using UHPC.[(8)] The design values for materials include compressive strength, first cracking strength, tensile strength, stress-strain relationships, modulus of elasticity, Poisson's ratio, thermal characteristics, shrinkage, creep, and fatigue. Other chapters address structural safety (strength design), serviceability, fatigue resistance, structural details, prestressed concrete, durability, construction (constituent materials, mix proportions, production, transportation, and inspection), cold-weather concreting, and hot weather concreting. The recommendations build on the Standard

Specifications for Concrete Structures prepared by the Japanese Society of Civil Engineers. Both recommendations and extensive commentary are provided.

For flexural design, the use of stress-strain curves rather than an equivalent stress block is recommended. No minimum amount of steel reinforcement is required because the bridging action of the steel fibers provides the strength after cracking.

Shear capacity is calculated as the summation of the shear resistance provided by the matrix, fiber reinforcement, and vertical component of the prestressing force or the shear resistance to diagonal compression failure. The use of shear reinforcement is not recommended. Torsional design is based on the Society's Standard Specifications. An equation is provided for the calculation of punching shear strength.

Serviceability is addressed by checks on stresses, displacements, deformations, vibrations, and other parameters as needed. Verification of fatigue resistance relies on the provisions of the Standard Specifications.

In pretensioned concrete, the clear vertical or horizontal distance between strands may be equal to the strand diameter. A minimum clear cover of 0.8 inches (20 mm) is permitted.

Overall, the document is comprehensive, although it defaults to the Standard Specifications where information is not available to develop different recommendations for UHPC.

AFGC-SETRA Recommendations

The French recommendations are composed of three parts. The first part provides specifications regarding the mechanical properties to be obtained, procedures to be used for placement, and checks and inspection during construction and of the finished product. The second part deals with the design and analysis of UHPC structures and accounts for the participation of fibers, nonprestressed reinforcement, and non-reinforced elements. The third part deals with durability of UHPC.

The first part provides design information for compressive strength, tensile strength, modulus of elasticity, Poisson's ratio, coefficient of thermal expansion, shrinkage, creep, and impact behavior. Mix design, mixing procedures, placement practices, and tests are addressed.

The design methods in the second part are based on the French codes for prestressed and reinforced concrete but take into account the strength provided by the fibers. The recommendations include an orientation coefficient that accounts for the alignment of fibers that may occur during placement. A minimum fiber content and non-brittleness check is also required. The stresses at the serviceability limit state are addressed in the same way as conventional reinforced or prestressed structures. When no prestressing steel or nonprestressed reinforcement is provided, a crack width criterion is used.

For the ultimate flexural strength limit state, the recommendations propose a stress-strain relationship that is linear for the compressive stress range but multilinear in the tensile stress range to account for the effect of the fibers.

At the serviceability limit state for shear, the recommendations use the shear stress limits of the French Code for prestressed concrete. Shear strength is calculated as the summation of the shear resistances provided by the concrete, reinforcement, and fibers.

The components of the third part address water porosity, oxygen permeability, chloride ion diffusion, portlandite content, stability of admixtures, delayed hydration, corrosion of steel fibers, and durability of polymer fibers.

More details on specific topics are provided in nine appendices. Feedback and research resulting from the use of the French recommendations have been summarized by Resplendino.

SUMMARY OF STRUCTURAL DESIGN

Limited testing under flexural or axial loads indicates that the flexural and axial strengths of UHPC members can be calculated with reasonable accuracy if the stress-strain relationships of UHPC are included in the analyses. However, the calculations are more complex than using the simplified approach of a rectangular compressive stress block and zero tensile strength.

The shear strength of UHPC beams containing conventional shear reinforcement and no steel fibers can be predicted using the sectional design method of the AASHTO LRFD Bridge Design Specifications. For UHPC beams with steel fibers and without conventional shear reinforcement, a strength calculation based on the maximum principal tensile stress has been used.

Where design for punching shear is required, the equations in ACI 318 may be used. For shear friction, the available test results need to be compared with the existing specifications.

The limited information available on torsion tests indicates that design could be performed using traditional mechanics of materials approach and limiting the maximum principal tensile stress.

For prestressed concrete, no stress limits or prestress loss values have been established for UHPC. The limited information on transfer length and development length of prestressing strand indicates that the lengths are much shorter in UHPC than in conventional concrete. Similarly, development lengths for deformed bars in tension and lap splices in tension are shorter than for conventional concrete.

For prestress losses, approximate estimates can be made using the modulus of elasticity, creep, and shrinkage data summarized in chapter 3.

Information on reinforcement details, standard hooks in tension, and development of welded wire reinforcement and shear reinforcement in UHPC members was not identified.

Three countries have developed design guidelines for use with UHPC. Although these documents are not as complete as the AASHTO LRFD Bridge Design Specifications, they do address the major design requirements.

CHAPTER 5. DURABILITY AND DURABILITY TESTING

INTRODUCTION

The use of UHPC in any infrastructure application requires the UHPC to have adequate resistance to deterioration caused by the environment to which it is exposed. This chapter reports on the durability of UHPC based on the parameters and tests generally used to determine the durability of conventional concrete.

PERMEABILITY

In the United States, the permeability of concrete is generally assessed using AASHTO T 277 (ASTM C1202)—Electrical Indication of Concrete's Ability to Resist Chloride Ion Penetration. Tests conducted by Graybeal in accordance with ASTM C1202 resulted in values of less than 40 coulombs at 28 days for steam-cured specimens and values of 360 and 76 coulombs at 28 and 56 days, respectively, for untreated specimens. Materials with values less than 100 coulombs are considered to have negligible chloride ion penetrability.

Ahlborn et al. reported rapid chloride permeability values of less than 100 coulombs for both air-cured and heat-treated concretes. Bonneau et al. reported values of 6 to 9 coulombs for two different mixes. Thomas et al. reported values of zero to 19 coulombs at an age of 28 days. Ozyildirim reported values of 19 and 35 coulombs.

Chloride penetration tests in accordance with AASHTO T 259 were also reported by Graybeal. This test involves ponding a 3-percent sodium chloride solution on the surface of the concrete for 90 days and then determining the penetration of the chlorides into the concrete. Although there tended to be higher levels of chloride ions near the surface, the amount of chloride that penetrated into the concrete was extremely small.

Different tests for permeability are used in other countries. One measure of chloride penetration is the value of its chloride diffusion coefficient. Reported values are as follows:

- 2×10^{-15} m^2/second in steady-state conditions and 3×10^{-11} m^2/second in non-steady-state conditions.
- 1.3×10^{-13} m^2/second at 28 days.
- 2.3×10^{-13} m^2/second in a non-steady-state condition.

Gao et al. tested the permeability of UHPC using pressure testing. No water leakage occurred when the hydraulic pressure was increased from 14.5 to 232 psi (0.1 to 1.6 MPa) at a rate of 14.5 psi (0.1 MPa) per 8 hours. After removing the pressure, moisture had penetrated 0.11 inches (2.7 mm) into the specimens.

The effects of microcracks induced by loading on chloride penetration have also been investigated. Graybeal examined the penetration of a 15-percent sodium chloride solution into the tension face of a beam. The beam was subjected to 500,000 cycles of repetitive loading

over 154 days to a maximum tensile stress 14 percent above the first cracking load. The solution penetrated to a depth of 0.12 inches (3 mm) on the side faces and 0.2 inches (5 mm) on the tensile face of the beam. The steel fibers crossing crack planes did not show any visible signs of section loss or tensile failure.

Aarup loaded small reinforced beams with a cover to the reinforcement of 0.4 inches (10 mm) to produce various levels of bending stresses. Over a period of 4 years, during which the beams were repeatedly exposed to a salt solution for 2 days and dried for 5 days, no correlation between loading of the beams and chloride diffusion was observed and no corrosion occurred. Measured diffusion coefficients for unloaded and loaded beams ranged from $2x10^{-14}$ to $1x10^{-15}$ m^2/second.

Charron et al. reported the results of permeability tests on UHPC specimens previously subjected to various levels of tensile deformation. Based on the test results, the maximum residual tensile strain whereby the water permeability remained low was determined to be 0.13 percent.

FREEZE-THAW RESISTANCE

The standard test for freeze-thaw resistance in the United States is AASHTO T 161 (ASTM C666)—Resistance of Concrete to Rapid Freezing and Thawing. AASHTO T 161 has two procedures. Procedure A involves rapid freezing and thawing in water while Procedure B involves rapid freezing in air and thawing in water. Tests of UHPC beginning 5 to 6 weeks after casting and using Procedure A were reported by Graybeal. Specimens subjected to steam curing prior to testing and untreated specimens showed very little deterioration throughout 690 cycles of freezing and thawing. The specimens that were untreated continued to hydrate and gain strength during the testing sequence.

The ability of conventional concrete to resist freeze-thaw damage can also be assessed by measuring certain parameters of its air-void system. Air-void analyses of UHPC reported by Graybeal are shown in table 13.

Table 13. Air-void system parameters

	Value	
Parameter	**inches**	**mm**
Voids	2.0 to 7.6/inches	0.08 to 0.30/mm
Specific surface	250 to 405 $inches^2/inches^3$	9.8 to 15.9 mm^2/mm^3
Spacing factor	0.009 to 0.027 inches	0.23 to 0.69 mm

Despite having an air-void system that might not be suitable with conventional concrete, the UHPC performed adequately in freeze-thaw testing.

Bonneau et al. reported that the durability factor of three different mixes was equal to or greater than 100 when tested using ASTM C666 Procedure A.

Acker and Behloul reported tests with 400 cycles of freezing and thawing that showed no degradation. Similar results were obtained by Ahlborn et al. and Piérard et al. Magureanu et al. reported that UHPC samples displayed higher values for compressive strength,

static modulus of elasticity, and dynamic modulus of elasticity after 1,098 freeze-thaw cycles compared with control specimens.

Based on their research, Müller et al. concluded that UHPC mixes show an extremely high freeze-thaw resistance to water with or without deicing salts. They attributed this to the very low moisture uptake by the UHPC.

SCALING RESISTANCE

The standard test for evaluation of scaling resistance in the United States is ASTM C672—Scaling Resistance of Concrete Surfaces Exposed to Deicing Chemicals. In this test, the surface is exposed to a salt solution and subjected to daily freeze-thaw cycles. Generally, 50 cycles are sufficient to evaluate a surface. Graybeal reported that after 215 cycles, no surface scaling of UHPC specimens had occurred. Bonneau et al. reported very low amounts of scaling for three mixes after 50 cycles.

Schmidt et al. reported a scaling rate of 100 g/m^2 (3 oz/yd^2) after 56 cycles of freezing and thawing compared with the normal acceptance limit for their test of 1,500 g/m^2 (44 oz/yd^2) after 28 cycles. Measurements of sound velocities showed no internal damage from freeze-thaw testing. Specimens that received no heat treatment showed a higher freeze-thaw resistance compared with heat-treated specimens.

Cwirzen et al. examined the effect of heat treatment on the durability of UHPC. The test results for specimens without steel fibers showed low surface-scaling values after 56 freeze-thaw cycles in all specimens. After 150 freeze-thaw cycles, the heat-treated specimens showed an increase in surface scaling. The relative dynamic modulus of the heat-treated specimens dropped below 50 percent after 200 cycles, whereas the non-heat-treated specimens showed a very small change. The presence of steel fibers restrained the internal damage but caused higher surface scaling.

CARBONATION

Carbonation of concrete is a process by which carbon dioxide from the atmosphere penetrates the concrete and reacts with various hydration products. Depth of carbonation is typically measured by applying phenolphthalein solution to the surface of the concrete and measuring the depth of the color change.

Small-scale beams of UHPC placed in a carbonation chamber and subjected to flows of 5- or 100-percent carbon dioxide showed no signs of carbonation after 2 years. On the other hand, Müller et al. reported that mechanically induced microcracks were observed to be partly or completely filled by carbonation.

Piérard et al. reported a carbonation depth of 0.006 to 0.008 inches (1.5 to 2.0 mm) after a 1-year exposure to a 1-percent CO_2 atmosphere. The duration of the test is generally limited to 56 days.

ABRASION RESISTANCE

Graybeal reported tests for the abrasion resistance of UHPC. The tests were conducted in accordance with ASTM C944—Abrasion Resistance of Concrete or Mortar Surfaces by the Rotating-Cutter Method on 6-inch (152-mm)-diameter cylinders that were cured using one of four curing methods. Three concrete surfaces were used—cast against a steel mold, sand blasted, and ground. The double test load was used. The results clearly indicated much higher abrasion resistance of steam-cured specimens compared with untreated specimens. For the steam-cured specimens, the surfaces cast against the steel mold had higher abrasion resistance than the sand-blasted or ground surfaces.

SULFATE RESISTANCE

Piérard reported no deterioration of UHPC when immersed in sodium sulfate solution for 500 days.

RESISTANCE TO ALKALI-SILICA REACTIVITY

Various tests to determine the resistance of concrete to alkali-silica reactivity (ASR) are available. ASTM C1260 contains a test procedure that accelerates any ASR reaction and can be accomplished in 16 days. Using a version of this test modified to allow for steam curing, Graybeal reported levels of expansion that were an order of magnitude below the threshold value for innocuous behavior. He concluded that there should be no concern about ASR with the UHPC that was tested. He noted that free water must be present for ASR to occur. With the low permeability of UHPC, it is unlikely that free water would be present.

MARINE EXPOSURE

Three series of UHPC mixtures were placed in a marine exposure site at Treat Island, ME. The exposure conditions included 20-ft (6-m) tides and more than 100 freeze-thaw cycles per year. After 5 to 15 years of exposure and more than 1,500 cycles of freezing and thawing in some cases, there was no evidence of deterioration or degradation of mechanical properties. The depth of chloride penetration was much lower than observed for typical HPC in the same environment.

FIRE RESISTANCE

Behloul et al. have reported information related to the fire resistance of UHPC made with Ductal-AF®. Ductal-AF® is specially formulated to have fire resistance. Published information includes the change in compressive strength, tensile strength, modulus of elasticity, thermal conductivity, specific heat, and coefficient of thermal expansion for specimens subjected to temperatures between 68 and 1,112 °F (20 and 600 °C).

Fire tests according to ISO 834 were also conducted on columns and beams using both loaded and unloaded specimens. Some specimens were steam cured while others were not. The authors reported that the results were very positive compared with conventional concrete when

using the French rules for fire safety. One feature was the lack of spalling that occurs with conventional concrete. This facilitated the use of thermal modeling to predict the behavior.

Heinz et al. reported the fire resistance of UHPC 3.9-inch (100-mm)-diameter cylinders and 4.7- by 9.4-inch (120- by 240-mm) columns under load. The concretes included either steel fibers or a combination of steel and polypropylene fibers. At an age of 24 hours, the specimens were heat treated in water at 194 °F (90 °C) for 24 hours. Testing followed the time-temperature curve of German standard DIN 4102-2. The cylinders without polypropylene fibers exhibited spalling after a few minutes. After 90 minutes, the sample was destroyed beyond recognition. In contrast, cylinders containing 0.66 percent by volume of polypropylene fibers showed no signs of spalling. However, cracks with widths of 0.012 to 0.02 inches (0.3 to 0.5 mm) were present over the whole surface of the cylinders. In testing the columns, spalling occurred after about 11 minutes. The initial period of spalling was followed by a dormant period with no further destruction until fracture of the specimens. The authors concluded that a UHPC with 3.05 percent by volume of steel fibers and 0.60 percent by volume of polypropylene provided the best results. The effects of elevated temperatures on the residual compressive strength and modulus of elasticity were also reported by Way and Wille.

Hosser et al. also conducted tests to evaluate which combinations of protective lining and polypropylene fiber content were able to minimize spalling under fire exposure.They also measured thermal conductivity and specific heat.

Aarup reported that the behavior of UHPC 1 week after fire tests was better than for conventional concrete. One reason stated for the improved performance was that the UHPC had a very high silica fume content and negligible calcium hydroxide content. A literature review of the behavior of UHPC at elevated temperatures has been prepared by Pimienta et al.

SUMMARY OF DURABILITY PROPERTIES

The dense matrix of UHPC prevents deleterious solutions from penetrating into the matrix, and so the mechanisms that can cause conventional concrete to deteriorate are not present. Consequently, durability properties, as measured by permeability tests, freeze-thaw tests, scaling tests, abrasion tests, resistance to ASR, and carbonation, are significantly better than those of conventional concrete. For fire resistance, it appears that a special formulation may be necessary.

CHAPTER 6. ACTUAL AND POTENTIAL APPLICATIONS

This chapter describes specific applications of UHPC in infrastructure projects. Separate sections contain descriptions of the applications in North America (United States and Canada), Europe, and Asia/Australasia. Potential applications described in the literature are also presented.

NORTH AMERICA

Table 14 provides a list of the applications in the United States and Canada.

Table 14. UHPC applications in North America

Name	Country	Year	Application	Reference (First Author)
Mars Hill Bridge, Wapello County, IA	United States	2006	Three 45-in.-deep bulb-tee beams	Bierwagon Endicott
Route 624 over Cat Point Creek, Richmond County, VA	United States	2008	Five 45-inch-deep bulb-tee girders	Ozyildirim
Jakway Park Bridge, Buchanan County, IA	United States	2008	Three 33-inch-deep pi-shaped girders	Keierleber
State Route 31 over Canandaigua Outlet, Lyons, NY	United States	2009	Joints between deck bulb tees	Shutt
State Route 23 over Otego Creek, Oneonta, NY	United States	2009	Joints between full-depth deck panels	Royce
Little Cedar Creek, Wapello County, IA	United States	2011	Fourteen 8-inch-deep waffle deck panels	Moore
Fingerboard Road Bridge over Staten Island Expressway, NY	United States	2011 to 2012	Joints between deck bulb tees	Royce
State Route 248 over Bennett Creek, NY	United States	2011	Joints between deck bulb tees	Royce
U.S. Route 30 over Burnt River and UPRR bridge, Oregon	United States	2011	Haunch and shear connectors and transverse joints	Bornstedt
U.S. Route 6 over Keg Creek, Pottawatomie County, IA	United States	2011	Longitudinal and transverse joints between beams	Graybeal
Ramapo River Bridge, Sloatsburg, NY	United States	2011	Joints between full-depth deck panels	Anon
State Route 42 Bridges (2) near Lexington, NY	United States	2012	Joints between full-depth deck panels and shear pockets	Anon

Name	Country	Year	Application	Reference (First Author)
State Route 31 over Putnam Brook near Weedsport, NY	United States	2012	Joints between full-depth deck panels	Anon
I-690 Bridges (2) over Peat Street near Syracuse, NY	United States	2012	Joints between full-depth deck panels	Anon
I-690 Bridges (2) over Crouse Avenue near Syracuse, NY	United States	2012	Joints between full-depth deck panels	Anon
I-481 Bridge over Kirkville Road near Syracuse, NY	United States	2012	Joints between full-depth deck panels	Anon
Windham Bridge over BNSF Railroad on U.S. Route 87 near Moccasin, Montana	United States	2012	Joints between full-depth deck panels and shear connections to beams	Anon
Sherbrooke Pedestrian Overpass, Quebec	Canada	1997	Precast, post-tensioned space truss	Blaise
Highway 11 over CN Railway at Rainy Lake, Ontario	Canada	2006	Joints between precast panels and shear connector panels	Perry
Glenmore/Legsby Pedestrian Bridge, Calgary	Canada	2007	Precast, post-tensioned tee-section	Perry
Highway 11/17, Sunshine Creek, Ontario	Canada	2007	Joint fill between adjacent box beams and between precast curbs	Graybeal
Highway 17, Hawk Lake, Ontario	Canada	2007 to 2008	Joint fill between adjacent box beams and between precast curbs	Graybeal
Sanderling Drive Pedestrian Overpass, Calgary	Canada	2008	Tee section drop-in girder	Anon
Highway 105 over Buller Creek, Ontario	Canada	2009	Joint fill between adjacent box beams and between precast curbs	Graybeal
Highway 71 over Log River, Ontario	Canada	2009	Joint fill between adjacent box beams and between precast curbs	Graybeal
Route 17 over Eagle River, Ontario	Canada	2010	Joint fill between adjacent box beams and between precast curbs and to establish live load continuity	Graybeal

Name	Country	Year	Application	Reference (First Author)
La Vallee River Bridge, Ontario	Canada	2010	Joint fill between adjacent box beams and between precast curbs	Graybeal
Highway 105 over Wabigoon River, Ontario	Canada	2010	Joint fill between adjacent box beams and between precast curbs	Graybeal
Highway 105 over the Chukuni River, Ontario	Canada	2010	Shear connector pockets and panel joints	Graybeal
Steel River Bridge on Highway 17, Ontario	Canada	2010	Shear connector pockets and panel joints	Anon
Mathers Creek Bridge on Highway 71, Ontario	Canada	2010	Joint fill between adjacent box beams and between precast curbs	Anon
Noden Causeway on Highway 11, Ontario	Canada	2010 to 2013	Joint fill between adjacent precast panels	Anon
Highway 17 over Current River, Ontario	Canada	2011	Joints between precast curbs	Perry
Mackenzie River Bridges (2) on Highway 11/17, Ontario	Canada	2011	Shear connector pockets and panel joints	Anon
Wabigoon River Bridge on Highway 605, Ontario	Canada	2011	Shear connector pockets and panel joints	Anon
Whiteman Creek Bridge on Highway 24, Ontario	Canada	2011	Shear pockets and longitudinal and transverse joints between precast panels. Connections between H-piles and precast abutments	Young
Shashawanda Creek Bridge, Ontario	Canada	2011	Shear connector pockets and longitudinal and transverse joints between precast panels	Anon
Hodder Ave Overpass over Highway 11/17, Ontario	Canada	2012	Joint fill between adjacent box beams and between precast curbs	Anon
Hawkeye Creek Bridge on Highway 589, Ontario	Canada	2012	Joint fill between adjacent box beams and between precast curbs	Anon

Name	Country	Year	Application	Reference (First Author)
Hawkeye Creek Tributary Bridge on Highway 589, Ontario	Canada	2012	Joint fill between adjacent box beams and between precast curbs	Anon
Black River Bridge on Highway 17, Ontario	Canada	2012	Joint fill between adjacent box beams and between precast curbs	Anon
Beaver Creek Bridge on Highway 594, Ontario	Canada	2012	Joint fill between adjacent box beams and between precast curbs	Anon
Middle Lake Bridge on Highway 17A, Ontario	Canada	2012	Joint fill between precast curbs and precast approach slabs	Anon
Jackpine River Bridge on Highway 17, Ontario	Canada	2013	Joint fill between adjacent box beams and between precast curbs	Young
Bug River Bridge on Highway 105, Ontario	Canada	2013	Joint fill between adjacent box beams and between precast curbs	Young
Beaver Creek Bridge on Highway 17, Ontario	Canada	2013	Joint fill between adjacent box beams and between precast curbs	Young
Sturgeon River Bridge on Highway 11, Ontario	Canada	2013	Joint fill between adjacent box beams and between precast curbs	Young
Blackwater River Bridge on Highway 11, Ontario	Canada	2013	Joint fill between adjacent box beams and between precast curbs	Young
Nugget Creek Bridge on Highway 17, Ontario	Canada	2013	Joint fill between adjacent box beams and between precast curbs	Young
Little Wabigoon Bridge on Highway 17, Ontario	Canada	2013	Joint fill between adjacent box beams and between precast curbs	Young
Melgund Creek Bridge on Highway 17, Ontario	Canada	2013	Joint fill between adjacent box beams and between precast curbs	Young
McCauley Creek Bridge on Highway 11, Ontario	Canada	2013	Joint fill between adjacent box beams and between precast curbs	Young

Name	Country	Year	Application	Reference (First Author)
Little Pic River Bridge on Highway 17, Ontario	Canada	2013	Shear connector pockets and panel joints	Young
Jackfish River Bridge on Highway 17, Ontario	Canada	2013	Shear connector pockets and panel joints	Young
Westminster Drive, Ontario	Canada	2014	Longitudinal joints to connect superstructure modules.	Young

The first highway bridge constructed in North America was the Mars Hill bridge in Wapello County, IA.[238] The simple single-span bridge, as shown in figure 13, comprises three 110-ft (33.5-m)-long precast, prestressed concrete modified 45-inch (1.14-m)-deep Iowa bulb-tee beams topped with a cast-in-place concrete bridge deck. Each beam contained forty-seven 0.6-inch (15.2-mm)-diameter, low-relaxation prestressing strands and no shear reinforcement.

Figure 13. Photo. Mars Hill Bridge, Wapello County, IA

One span of the 10 spans of the Route 624 bridge over Cat Point Creek in Richmond County, VA, was built using UHPC. (See figure 14.) Bulb-tees with a depth of 45 inches (1.14 m) and a length of 81 ft 6 inches (24.8 m) were used. The specified compressive strengths were 12.0 ksi (83 MPa) at release of the strands and 23.0 ksi (159 MPa) for design. The beams did not contain any nonprestressed shear reinforcement.

Figure 14. Photo. Route 64 over Cat Point Creek, Richmond County, VA

Following extensive research and testing by FHWA, a UHPC bridge using pi-shaped girders was constructed in Buchanan County, IA, in 2008. (See figure 15.) The shape is named after the Greek letter. The cross section, shown in figure 16, is similar to a double-tee section but with bottom flanges on the outside of each web. Three pi-girders were used in the central 51-ft 4-inch (15.6-m)-long center span of the three-span bridge.

Figure 15. Photo. Jakway Park Bridge, Buchanan County, IA

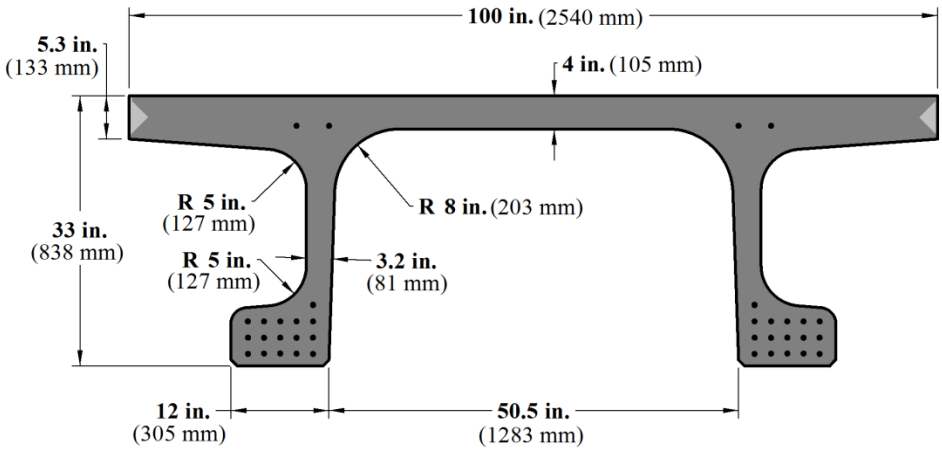

Figure 16. Illustration. Cross section of pi-shaped girder

In New York State, several bridges have been built using field-cast UHPC to create connections between adjacent precast concrete elements. (See figure 17.) These applications take advantage of the short development lengths that can be used for splice lengths of nonprestressed reinforcement in UHPC. The same technique was used on the transverse joints over the piers of the Keg Creek Bridge, IA, to establish continuity for live load and in the longitudinal joints between deck panels. The use of UHPC in the construction of connections is described by Graybeal.

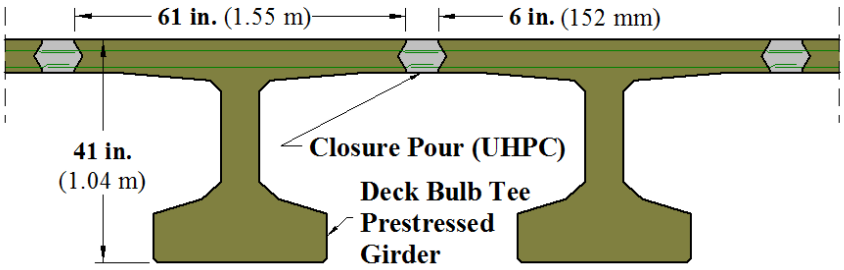

Figure 17. Illustration. Cross section showing CIP UHPC connection between precast beams

Little Cedar Creek in Wapello County, IA, used 14 UHPC waffle panels for the deck on a 60-ft (18.3-m)-long 33-ft (10.0-m)-wide concrete bridge. The panels were 15 ft by 8 ft by 8 inches deep (4.6 m by 2.4 m by 203 mm deep) at the deepest point, with the waffle squares having a thickness of only 2.5 inches (64 mm). All connections between adjacent panels and from panels to the precast, prestressed concrete beams used UHPC.

The first bridge to use UHPC in Canada was the pedestrian/bikeway bridge in Sherbrooke, Quebec, as shown in figure 18. The structural concept consists of a space truss with a top UHPC chord that serves as the riding surface, two UHPC bottom chords, and truss diagonals that slope in two directions. Each diagonal consists of UHPC confined in 6-inch (152-mm)-diameter stainless steel tubes. The bridge was constructed from six prefabricated match-cast segments with two half-spans assembled prior to erection across the river to create a 197-ft (60-m)-long span.

Figure 18. Photo. Pedestrian bridge, Sherbrooke, Quebec, Canada

Other bridges in Canada that have used UHPC are listed in table 14. The applications include longitudinal and transverse joints between precast components, shear connector pockets between beams and slabs, and a precast post-tensioned tee section for a pedestrian bridge. See Figure 19. Most of the applications have been in Ontario with leadership by the Ministry of Transportation.

Figure 19. Photo. Glenmore/Legsby pedestrian bridge, Calgary, Alberta, Canada

EUROPE

UHPC has been used in bridges in Austria, Croatia, France, Germany, Italy, the Netherlands, Slovenia, and Switzerland as listed in table 15.

Table 15. UHPC applications in Europe

Name	Country	Year	Application	Reference (First Author)
WILD bridge, Völkermarkt	Austria	2010	Arch bridge with five straight chords	Freyta He
Bakar bridge	Croatia	—	Arch bridge	Čandrlić
Sermaises footbridge	France	—	U-shaped footbridge with a 30-min fire rating	Behloul
Bourg-Les-Valence overpass bridges (2)	France	2001	Pi-shaped beams (double tee)	Hajar
PS 34 overpass on the A51 Campenon Bernard	France	2005	Precast, post-tensioned segmental single cell box girder	Resplendino
Sainte Pierre La Cour bridge, Mayenne	France	2005	Precast, prestressed I-beams and deck panels	Resplendino
Pinel bridge, Rouen	France	2007	Prestressed beams	de Matteis
Pont du Diable footbridge	France	2008	Prestressed beams and deck to form a U-shape	Behloul
TGV East High Speed Line, aqueduct	France	—	Post-tensioned U-shape	Resplendino
Angels footbridge, Herault	France	—	221-ft span, 5.9 ft-deep section	Resplendino
Pedestrian/cycle track Niestetal	Germany	—	Post-tensioned trough section	Fehling
Gaertnerplatz bridge, Kassel	Germany	2007	Variable depth space truss	Fehling
Obertiefenbach	Germany	2007	Waterproofing layer and hinge	Kim
Friedberg	Germany	2007	Pi-shaped beam	Fehling
Weinheim	Germany	2007	Pi-shaped beam	Fehling
—	Italy	—	Bridge	Meda
Rehabilitation of orthotropic bridge deck, Caland	Netherlands	—	Toppings and deck panels	Buitelaar Yuguang
Kaag bridges, Sassenheim	Netherlands	2002	Deck panels	Kaptijn

Name	Country	Year	Application	Reference (First Author)
Log Cezsoski bridge	Slovenia	2009	Bridge deck overlay	Sajna
Luaterbrunnen footbridge	Switzerland	—	Flooring	Resplendino
Single span road bridge	Switzerland	2004	Rehabilitation and widening of a bridge deck	Brühwiler
Crash barrier repair	Switzerland	2006	Protective surface layer	Brühwiler
Bridge pier repair	Switzerland	2007	Precast panels for a protective layer	Brühwiler
Various	Various	—	Repair and strengthening	Resplendino

— Construction date is unknown.

The Bourg-Les-Valence bridges in France are claimed to be the first UHPC road bridges. Each bridge consists of two spans made continuous with a CIP UHPC connection between spans. The cross section consists of five spliced pretensioned beams that resemble a double-tee with the addition of bottom flanges similar to a pi-shaped section. Beam lengths are 67.3 and 73.8 ft (20.5 and 22.5 m). The only nonprestressed reinforcement is provided where the components are joined together longitudinally or transversely and at locations of attachments. UHPC was used in the longitudinal joints between beams.

The PS34 Overpass on the A51 motorway in France is a precast, post-tensioned, single-cell box girder bridge with a length of 155.5 ft (47.4 m). The cross section has a constant depth of 63 inches (1.60 m), a top slab thickness of 5.5 inches (140 mm), and web and bottom slab thickness of 4.7 inches (120 mm). The bridge is post tensioned longitudinally with six external tendons.

The St. Pierre La Cour bridge in France consists of 10 UHPC precast, prestressed concrete I-beams spaced at 55-inch (1.395-m) centers with a simple span length of 62.3 ft (19 m). The deck consists of 1-inch (25-mm)-thick UHPC precast panels and an 8-inch (200-mm)-thick CIP deck.

According to Fehling, the first UHPC bridges in Germany were built in Niestetal near Kassel with span lengths of 23.0, 29.5, and 39.4 ft (7, 9, and 12 m). The longest span used a shallow trough section and was post tensioned. The other two spans used a pi-shaped section and were pretensioned. Two other bridges using the pi-shaped cross-section were built near Friedberg and Weinheim with span lengths of 39.4 and 59.0 ft (12 and 18 m), respectively.

The Gaertnerplatz bridge, a pedestrian/bicycle bridge across the Fulda River in Kassel, Germany, is a six-span structure with a total length of 437 ft (133.2 m) and a main span of 118 ft (36 m). The structural system is a variable-depth space truss consisting of two top UHPC chords and a single bottom tubular steel chord. The diagonal tubular steel chords are inclined

both longitudinally and transversely. The deck spans between and cantilevers beyond the two top chords for a total width of 16.4 ft (5 m). Its thickness varies from 3.1 to 3.9 inches (80 to 100 mm). The deck is glued to the top chords.

In Slovenia, a bridge deck was overlaid with 1 to 1.2 inches (25 to 30 mm) of UHPC. An inspection 2 years after installation showed no damage, cracks, or spalling. Applications in Switzerland include rehabilitation and widening of an existing bridge, protection layers to repair a crash barrier and bridge piers, and flooring for a footbridge.

ASIA AND AUSTRALASIA

UHPC applications for highway infrastructure in Australia, Japan, Malaysia, New Zealand, and South Korea are listed in table 16. Descriptions of some of these bridges are provided below.

Table 16. UHPC applications in Asia and Australia

Name	Country	Year	Application	Reference (First Author)
Shepherds Creek Road bridge, New South Wales	Australia	2005	Precast, pretensioned I-beams	Rebentrost Anon Cavill
Yarra River bridge	Australia	2008 to 2009	Noise barrier protection panels	Anon
Kuyshu Expressway bridge	Japan	—	—	Okuma
Riverside Senshu footbridge, Nagaoka-shi	Japan	—	Three-span continuous structure	Matsubara
Sakata-Mirai footbridge, Sakata	Japan	2002	Post-tensioned box girder	Rebentrost Resplendino Tanaka[276]
Akakura Onsen Yukemuri pedestrian bridge	Japan	2004	Prestressed U-shaped girder	Tanaka[276]
Yamagata	Japan	2004	Box girder	Rebentrost
Tahara bridge Aichi	Japan	2004	Box girder	Rebentrost
Horikoshi Highway C-ramp Fukuoka	Japan	2005	Composite I-girder	Rebentrost Tanaka
Keio University footbridge, Tokyo	Japan	2005	Pretensioned slab	Rebentrost Tanaka
Torisaka, River Highway bridge, Hokkaido	Japan	2006	Launching nose	Rebentrost
Toyota City Gymnasium footbridge, Aichi	Japan	2007	Box girder	Tanaka

Name	Country	Year	Application	Reference (First Author)
Sankin-ike footbridge, Fukuoka	Japan	2007	Box girder	Rebentrost
Hikita pedestrian bridge, Tottori	Japan	2007	U-shaped girder	Rebentrost
Haneda Airport Runway D, Tokyo	Japan	2007	Precast, pretensioned slabs	Rebentrost Tanaka
Mikaneike footbridge. Fukuoka	Japan	2007	U-shaped girder	Musha
Kobe Sanda premium outlet footbridge	Japan	2008	U-shaped girder	Tanaka
Akasaka Yogenzaka footbridge	Japan	2009	U-shaped girder	Tanaka
Torisalogawa bridge	Japan	2006	Box girder	Tanaka
Tokyo Monorail	Japan	2007	U-girder upside down	Tanaka
GSE bridge Tokyo Airport	Japan	2008	U-girders	Tanaka
Kampung Linsum bridge Rantau, Negeri Seremban	Malaysia	—	U-beam	Lei Voo
Sungai Muar bridge	Malaysia	—	Curved saddles for cable stays	Resplendino
Papatoetoe footbridge	New Zealand	2005	Pi-beam	Anon
Five pedestrian bridges, Auckland	New Zealand	2006 to 2007	Precast, post-tensioned Pi-girder	Rebentrost Anon
Seonyu Sunyudo footbridge, Seoul (Peace Bridge)	South Korea	2002	Precast, post-tensioned pi-section	Rebentrost Resplendino
Office pedestrian bridge	South Korea	2009	Cable-stayed bridge	Kim

— Data are unknown.

The Shepherds Creek bridge in Australia is a single 49-ft (15-m)-span bridge with a 16-degree skew. The superstructure consists of sixteen 23.6-inch (600-mm)-deep precast, prestressed UHPC beams spaced at 51 inch (1.3 m) centers. These support 1-inch (25-mm)-thick precast UHPC panels and a 6.7-inch (170-mm)-thick CIP reinforced concrete deck.

Numerous bridges, as listed in table 16, have been constructed in Japan beginning with the Sakata-Mirai bridge in 2002. (See figure 20.) This footbridge consists of pretensioned box girder segments that were post tensioned together to form a single span of 161 ft (49.2 m).

Most of the UHPC footbridges in Japan consist of precast segmental U-beams with a separate top slab that is integrally connected to the U-beam. The U-beam segments are connected longitudinally with a CIP joint and post tensioning.

The Horikoshi Highway C-Ramp bridge was Japan's first highway bridge using UHPC. The composite girder bridge is composed of four pretensioned UHPC I-shaped girders and a conventional CIP concrete deck. The use of UHPC in the girders allowed reduction of the number of girders from 11 to 4. The weight of each girder was less than it would have been with conventional concrete, allowing the use of a smaller crane. The overall weight of the bridge was reduced by 30 percent.

Figure 20. Photo. Sakata-Mirai bridge, Sakata, Japan

The Toyota Gymnasium footbridge is a two-cell segmental box girder using match-cast segments and dry joints with epoxy. To overcome the shortening caused by autogenous shrinkage of the lead segment before casting the next segment, a steel plate was used at the end of the lead segment and becomes the end form for the new segment.

The construction of Runway D at Tokyo's Haneda International Airport used 9.8-inch (250-mm)-deep UHPC panels spanning between longitudinal steel girders above the Tamar River.The panels consist of ribs supporting a slab with a minimum thickness of 3 inches (75 mm). This reduced the dead load of the slab by about 56 percent compared with conventional concrete. Approximately 6,900 panels were produced for this application.

The Sunyudo (Peace) footbridge in South Korea is an arch bridge with a main span of 394 ft (120 m).(See figure 21.) It is built from six precast, post-tensioned pi-shaped sections 4.3 ft (1.30 m) deep. The upper flange is a ribbed slab 1.19 inches (30 mm) thick with transverse prestressing. The webs of the pi-shaped section are 6.35 inches (160 mm) thick and inclined outward at the bottom. The six precast sections are post tensioned together by tendons located in the upper and lower haunches of the section. This bridge is the longest span UHPC bridge in the world.

Figure 21. Photo. Footbridge of Peace, Seoul, South Korea

REALIZED AND POTENTIAL SECURITY APPLICATIONS

Significant research and development efforts have also occurred with regard to the potential security applications afforded by UHPC. Infrastructure security can be a critical consideration, thus leading to opportunities to use UHPC components either as barrier protection systems or as inherent portions of the critical infrastructure. A state-of-the-art report on fiber-reinforced UHPC with a focus on security applications was completed in 2010.

Research on the mechanical properties of UHPC when subjected to high strain rate loading has been completed by Parent et al., Ngo et al., Millard et al., Habel and Gauvreau, and Millon et al. Blast resistance testing has been reported by Wu et al., Ngo et al., and Rebentrost and Wight. Penetration resistance tests have been reported by Rebentrost and Wight and by Nöldgen et al.

OTHER POTENTIAL APPLICATIONS

This section identifies other potential applications found during the literature search.

Almansour and Lounis compared the design of a prestressed concrete girder bridge using either UHPC or HPC in the girders. The design of the UHPC bridge was based on a combination of the Canadian Highway Bridge Design Code (CHBDC) and the AFGC-IR-02. The design of the HPC bridge was based only on the CHBDC. Both bridges had a span length of 147.6 ft (45 m). Five girders with a depth of 63 inches (1,600 mm) were required for the HPC bridge, and only four girders with a depth of either 35.4 inches (900 mm) or 47.2 inches (1200 mm) were required for the UHPC bridge. The 47.2-inch (1,200-mm)-deep girders represented a conservative design, whereas the shallower sections required more prestressing strands. An optimum solution would be a girder with a depth between 35 and 47 inches (900 and 1,200 mm).

The design of a pilot project for a 39-ft (12-m) span pedestrian bridge using composite steel-concrete construction was reported by Jungwith et al.

Obata et al. examined the use of prefabricated UHPC panels 1.2 inches (30 mm) thick as an overlay for asphalt pavement. The panels were bonded to the asphalt using a grout. About 517 ft^2 (48 m^2) of test pavement was constructed at a test track in Japan using different construction bonding procedures. No cracks were observed before load testing began. Delaminations occurred and increased with the number of wheel passes in some test sections. The authors concluded that early opening of the pavement to traffic is possible with the use of high-strength fast-curing grout.

Oesterlee et al. performed finite element analyses of a conceptual bridge girder using UHPC as an overlay material in place of a conventional waterproofing membrane. The structural response under combined loading from restrained shrinkage and traffic loads showed stresses close to the elastic tensile strength of the UHPC overlay where there was a high degree of restraint. The risk of transverse cracking in the overlay was deemed unlikely.

Schafers and Seim described theoretical and experimental investigations into the composite behavior of UHPC decks on timber beams. They conducted shear tests of the glued joint between the UHPC and timber to identify the best adhesives and timber surface preparation methods.

Using finite element modeling and experimental verification, Toutlemende et al. investigated the possible use of UHPC precast ribbed waffle slabs for a bridge deck. The slabs were pretensioned in the transverse direction and then post tensioned longitudinally before being connected to the longitudinal steel girders. The test results were compared with analytical models.

Vande Voort et al. explored the use of UHPC in H-shaped precast, prestressed concrete piles. They used laboratory tests to verify moment-curvature response. Two piles were successfully driven into clay soils and tested under vertical and lateral loads. (See figure 22.) The impact resistance of UHPC for use in piles was investigated by Leonhardt et al.

Figure 22. Photo. Experimental precast pile made of UHPC

Other potential applications that have been investigated are listed in table 17.

Table 17. Other potential applications of UHPC

Application	Reference (First Author)
Drill bits for special foundation engineering	Ibuk
Sewer pipes	Schmidt
Precast spun columns and poles	Adam, Müller
Barrier walls	Young
Field-cast thin-bonded overlays	Young, Sritharan, Shann, Schmidt, Scheffler
Cable-stayed bridge superstructure	Kim, Park
Bridge bearings	Hoffmann
Precast tunnel segments	Randl
Seismic retrofit of bridge columns	Massicotte

CHAPTER 7. FUTURE DIRECTION

This state-of-the-art report identifies the following four primary characteristics of UHPC that distinguish it from conventional concrete:

- Higher compressive strength.
- Higher tensile strength with ductility.
- Increased durability.
- Higher initial unit cost.

The compressive strength of UHPC makes it an ideal material for use in applications in which compressive stress is the predominant design factor. The ductility in tension allows the tensile strength of UHPC to be considered in both service and strength design for flexure, shear, and torsion. The durability of UHPC makes it an ideal material for use in an outdoor or severe exposure environment. The higher initial unit cost means that its use needs to be optimized for the intended application and that greater attention should be given to life-cycle costs. In addition, specifiers should consider all costs associated with the use of UHPC on a project, not just the material unit cost. In many cases, the use of UHPC may allow a redesign of the structure thus affecting many aspects of the total cost of deploying the structure. For example, the ability to omit shear reinforcement in a beam can result in a savings of both materials and labor that must be considered alongside the increased material costs. Nevertheless, a number of challenges must be overcome to achieve wide-scale implementation in the U.S. highway infrastructure. These are outlined in the following sections.

OWNER ISSUES

One of the primary advantages of UHPC to owners is its long-term durability. As discussed in chapter 5, the measured durability characteristics far exceed those of conventional concrete. These characteristics should result in structures with a longer service life compared with structures built with conventional concrete, and thus could potentially decreased life-cycle costs. No studies were identified for this report to show that this is the case. When owners began to consider the use of high-strength concrete in bridge beams, a clear case could be made that the initial cost would be less because the number of beams for a given bridge would be reduced. This may not be true with UHPC because the cost differential between conventional concrete and UHPC is much greater than it was between conventional concrete and high-strength concrete. Studies are needed to illustrate the cost benefits of using UHPC for bridges in the United States.

The number of demonstration projects in the United States is limited, with most occurring in only two States. For owners to obtain a reasonable level of comfort in using UHPC, more demonstration projects are needed, and the results need to be disseminated through a variety of channels. These include webinars, in-house seminars, technical symposia, and technical publications. Some of this activity has been ongoing for the past 10 years but more is needed. This is not just for owners but also for bridge designers, contractors, and producers.

There are, however, situations where UHPC can be used to address certain performance issues without a major cost impact. One example is the use of UHPC to fill the connection regions

between adjacent prefabricated elements. In this application, the overall cost increment in using UHPC is small because the quantity of material is small. The use of UHPC is reported to eliminate the cracking and leakage that occurs when conventional concretes or grouts are used. At the same time, the use of UHPC can enable the deployment of simplified connection details with shorter discrete reinforcement splice lengths and a reduced number of conflict points.

DESIGN ISSUES

The literature search identified the following national design and construction recommendations for UHPC:

- Design Guidelines for Ductal Prestressed Concrete Beams (Australia).
- Recommendations for Design and Construction of Ultra High Strength Fiber Reinforced Concrete Structures by the Japan Society of Civil Engineers.
- Ultra High Performance Fibre-Reinforced Concretes, Interim Recommendations prepared by AFGC (French Association of Civil Engineers) and SETRA (French Road and Traffic Government Agency (SETRA-AFGC 2002).

These documents are generally based on the primary document used for bridge design in the individual country. Where sufficient information is not available to support a change or a change is not necessary for UHPC, the documents resort to the provisions of the primary document.

For UHPC to gain greater use in the U.S. highway infrastructure, a design and construction document based on the AASHTO LRFD Bridge Design Specifications and the AASHTO LRFD Bridge Construction Specifications is needed. The lack of this document has led to the need to consider each project individually. In most cases, the design has been accepted based on structural tests rather than a rational design basis. A guide specification for construction with UHPC will help owners implement the technology.

Although more research is desirable, it is likely that sufficient information exists today to develop a document addressing the major aspects of structural design according to U.S. practices. These design aspects include material properties, flexural and axial load, tensile load, shear, transfer and development length of prestressing strand, approximate estimates of time-dependent losses based on creep and shrinkage data, some aspects of reinforcement details, and durability. Where information is lacking, the document could use the provisions of the existing bridge specifications. This concept may not immediately result in the most economical design but will generally be conservative. Because several demonstration projects have been completed in the United States, there should be sufficient experience available to identify the necessary provisions in a construction guide specification.

For proper implementation of UHPC, new test procedures that address UHPC are needed for both development of mixes and quality control of the fresh and hardened UHPC. In most cases, these can be adaptations of existing test standards for conventional concrete but modified for the

particular properties of UHPC. In addition, generic material specifications are needed to encourage the introduction of competitive materials.

PRODUCTION ISSUES

At the present time, very few producers have experience with UHPC for precast or cast-in-place applications. Information needs to be made available so that they are aware of the differences to expect with UHPC. For example, precasters need to be aware of the need for longer mixing times in conventional concrete mixers, longer set times, and modified curing regimes. Quality control tolerances need to be defined for the standard test methods. For example, the use of small-size cylinders for measurement of compressive strength needs to be established, along with the requirements for specimen preparation and testing machine capabilities.

RESEARCH NEEDS

The largest general design topic area where research is lacking concerns reinforcement details for nonprestressed reinforcement and prestressing strands. This includes development of and splice lengths of bars in tension and compression. Although the existing provisions for conventional concrete could be used, they do not take advantage of the enhanced tensile and compressive strengths of UHPC. A systematic investigation of strand spacing and strand cover is needed for 0.5-, 0.6-, and 0.7-inch (12.7-, 15.2-, and 17.8-mm)-diameter strands to determine whether decreased spacing can be used with UHPC.

Investigations into the use of and reliance upon fiber reinforcement in structural concrete members is also needed. Fiber type, geometry, volume, dispersion, and orientation can all affect the structural performance of the concrete member. Development of interrelated material proportioning methods, component fabrication methods, and structural design concepts are recommended.

U.S. Federal law requires compliance with Buy America provisions. Research is needed into the use of either domestically produced steel fibers and/or the use of non-steel fibers while still producing a UHPC-class material that affords appropriate characteristics.

SUMMARY OF NEEDS

To encourage greater implementation of UHPC in the highway infrastructure, the following activities and documents are needed in approximate order of priority:

- Studies showing the cost effectiveness of UHPC in various applications.
- Design and construction guide specifications for structures made with UHPC.
- Research to address some of the missing information needed in the structural design guidelines.
- Standard test methods and material specifications for UHPC.

- Production procedures for precast and cast-in-place construction.
- Broader geographic distribution of demonstration projects.
- Ongoing and greater distribution of technical information.

AASHTO and FHWA should consider the development of structural design and construction guidelines. This effort should include research to address some of the needed missing information. The current efforts to engage organizations such as the American Concrete Institute, the Precast/Prestressed Concrete Institute (PCI), and ASTM should be extended to AASHTO. PCI should work to develop production procedures for precast UHPC products. The National Ready Mixed Concrete Association should endeavor to address hurdles related to cast-in-place UHPC production, delivery, and casting. The involvement of the AASHTO Highway Subcommittee on Materials and ASTM Committees C09 on Concrete and Concrete Aggregates and C01 on Cement would facilitate the development of test methods and material specifications. The availability of funding to support these activities would accelerate the process.

The need for broader geographic distribution of demonstration projects should be addressed by FHWA in cooperation with the State departments of transportation.

Finally, and perhaps most important, owners need to be convinced that the use of UHPC is a good investment. Without that justification and the resulting demand, UHPC will remain a niche product.

1. **What is the primary characteristic of Ultra-High Performance Concrete (UHPC)?**
   - High workability
   - High compressive and tensile strength
   - Low density
   - Minimal curing time

2. **UHPC typically contains which of the following materials?**
   - Coarse aggregates
   - Steel fibers
   - Expanded clay
   - Wood fibers

3. **What is the primary benefit of UHPC in bridge construction?**
   - Reduced weight
   - Increased durability and strength
   - Faster construction time
   - Reduced labor costs

4. **In which year did the Federal Highway Administration (FHWA) begin investigating UHPC for infrastructure?**
   - 1995
   - 1997
   - 2001
   - 2005

5. **What is the minimum compressive strength classification for UHPC?**
   - 5 ksi
   - 10 ksi
   - 15 ksi
   - 21.7 ksi

6. **Which of the following countries was one of the first to construct a UHPC bridge?**
   - Canada
   - Germany
   - Japan
   - United States

7. **Which of the following curing methods enhances the mechanical properties of UHPC the most?**
   - Air curing
   - Steam curing at high temperatures
   - Water curing
   - UV exposure

8. **UHPC's enhanced durability is due to:**
   - The use of synthetic aggregates
   - The presence of micro-cracks
   - A discontinuous pore structure
   - High permeability

9. **Which of the following is NOT a common application of UHPC?**
   - Precast bridge girders
   - Pavement surfacing
   - Bridge deck panels
   - Jointing material

10. **The tensile strength of UHPC is typically measured using:**
    - Standard compressive cylinder tests
    - Direct tension tests
    - Water absorption tests
    - Workability tests

11. **What is the role of steel fibers in UHPC?**
    - To increase workability
    - To improve tensile strength and crack resistance
    - To reduce the weight of the concrete
    - To enhance thermal insulation

12. **Which of the following factors influences the mechanical performance of UHPC the most?**
    - Color of the cement
    - Fiber orientation and dispersion
    - Water temperature during mixing
    - Air temperature

13. What is one major environmental consideration associated with UHPC production?

- High energy demand for material production
- Excessive water usage
- Limited availability of raw materials
- High carbon sequestration potential

14. How does UHPC compare to conventional concrete in terms of permeability?

- Higher permeability
- Lower permeability
- No difference
- Highly dependent on curing method

15. Which of the following is an advantage of UHPC in structural applications?

- Higher fatigue resistance
- Increased air content
- Higher slump value
- Lower material cost

16. What is the typical modulus of elasticity for UHPC?

- 6,000 - 7,500 ksi
- 10,000 ksi
- 15,000 ksi
- 25,000 ksi

17. What is a unique property of UHPC under high temperatures compared to conventional concrete?

- Partial strength recovery upon cooling
- Higher thermal expansion
- Reduced heat resistance
- Increased water absorption

18. Which factor is least likely to impact the long-term performance of UHPC in bridge applications?

- Moisture exposure
- Concrete color
- Freeze-thaw cycles
- Fire resistance

19.The flexural behavior of UHPC is primarily influenced by:

Cement type
Fiber reinforcement and distribution
Water-cement ratio
Silica fume content

20.Which of the following tests is often used to assess UHPC workability?

Flow table test (ASTM C1437)
Slump test (ASTM C143)
Water absorption test
Penetration resistance test